
MASTER THESIS

# An effective forces study of polarized asymmetric nuclear matter

*Author:*
Alejandro ROMERO ROS

*Supervisors:*
Dr. Artur POLLS MARTÍ
Dr. Bruno JULIÁ-DÍAZ


UNIVERSITAT DE BARCELONA

Dep. Física Quàntica i Astrofísica
Facultat de Física
Universitat de Barcelona

July 25, 2017

# *Acknowledgements*

I would like to sincerely thank my advisors, Dr. Artur Polls and Dr. Bruno Juliá-Díaz, for their constant help and support on the fulfilment of this project. Also, I would like to thank my friends and family for their companion and enlivenment.

# Contents

# Chapter 1

# Effective Forces

The properties of homogeneous nuclear and neutron matter at high densities play a crucial role in the determination of the structure of neutron star interiors [1, 2, 3]. Terrestrial nuclei do not provide enough information to constrain an equation of state (EoS) under the extreme conditions of density and isospin asymmetry, and also a possible spin polarization that we can find inside neutron stars. Thus, a potentially safe way to obtain the EoS relies on microscopic many-body calculations based on realistic nucleon-nucleon (NN) interactions [4].

These realistic NN interactions should fulfil a minimum set of requirements. In particular, realistic potentials are build to reproduce the Nijmegen database [5], which contains a full set of NN elastic scattering phase-shifts up to energies of about $350\,\mathrm{MeV}$ and also to reproduce the properties of the only two nucleon bound state: the deuteron, which is bound by $2.22\,\mathrm{MeV}$ in the partial wave ${}^3S_1 - {}^3D_1$.

In principle, the realistic interactions are the apppropiate ones to be used in the so called *ab initio* many-body calculations, which aim at providing a first-principles description of the EoS of symmetric nuclear matter and neutron matter.

The NN interactions fulfilling these minimum requirements have a notorious complexity and depend on the spin and isospin degrees of freedom of the NN system. In particular, the tensor dependence, which is the direct responsible of the coupling between the ${}^3S_1$ and ${}^3D_1$ partial waves in the deuteron, increases the complexity of the problem.

Several many-body techniques have been developed to deal with these realistic interactions. Due to the strong repulsion present in any realistic interaction, they require the use of correlated wave functions or the sum of infinite perturbative diagrams (ladder diagrams) [6]. The large complexity of the calculations and the NN interactions themselves make very convenient the use of effective NN interactions, which are commonly implemented in the Hartree-Fock approximation and, therefore, easier to treat. Although effective forces have successfully been used in both finite nuclei and nuclear matter, they do not reproduce the phase-shifts nor the properties of the deuteron.

By construction, most of the effective forces used in the literature are well behaved around the saturation density of nuclear matter and for moderate isospin asymmetries. In general, these effective interactions depend on a set

of parameters that are determined by reproducing basic properties of symmetric nuclear matter as the saturation density $\rho_0$, the binding energy $e_0(\rho_0)$, the incompressibility modulus $\kappa(\rho_0)$ and the symmetry energy $e_{sym}(\rho_0)$ together with the binding energy of some double magic nuclei [7].

Once a parametrization is determined, one can, for instance, study nuclei and nuclear matter under conditions far from those used to define the force, in quite a simple way. When doing so, however, one must always keep in mind the particular limitations of the parametrization that has been using.

In this work, we will use two types of effective interactions: the Skyrme interaction [8, 9], that has a zero-range character and a simple spin-isospin dependence, and the Gogny interaction [10], which besides a zero-range term has finite-range terms of Gaussian shape along with a spin-isospin dependence.

The main objective will be to build the Hartree-Fock framework to calculate single-particle potentials and total energy per particle of polarized asymmetric nuclear matter and explore the possible spin instabilities of nuclear and neutron matter with effective forces constructed using conditions of zero spin polarization.

## 1.1 The Skyrme interaction

The Skyrme forces where introduced by T. H. R. Skyrme [8] around 1950 and, since the pioneering work of Vautherin and Brink [9], there has been an intensive and successful use of Skyrme effective NN interactions [11, 12]. They are characterized by a zero-range interaction (contact interactions) that leads to simple analytical expressions for basic properties of nuclear matter such as the ones we have already mentioned (binding energy, incompressibility modulus, saturation density and symmetry energy). A Skyrme force has the following structure:

$$\begin{aligned}\hat{v}_{Sk}(\mathbf{r}) =& t_0(1+x_0\hat{P}_\sigma)\delta(\mathbf{r}) \\ &+\frac{1}{6}t_3(1+x_3\hat{P}_\sigma)[\rho(\mathbf{R})]^\gamma\delta(\mathbf{r}) \\ &+\frac{1}{2}t_1(1+x_1\hat{P}_\sigma)\Big[\delta(\mathbf{r})\mathbf{k}'^2+\mathbf{k}^2\delta(\mathbf{r})\Big] \\ &+\frac{1}{2}t_4(1+x_4\hat{P}_\sigma)\Big[\delta(\mathbf{r})\rho(\mathbf{R})\mathbf{k}'^2+\mathbf{k}^2\rho(\mathbf{R})\delta(\mathbf{r})\Big] \\ &+t_2(1+x_2\hat{P}_\sigma)\mathbf{k}'\delta(\mathbf{r})\mathbf{k}+t_5(1+x_5\hat{P}_\sigma)\mathbf{k}'\rho(\mathbf{R})\delta(\mathbf{r})\mathbf{k} \\ &+iW_0(\boldsymbol{\sigma}+\boldsymbol{\sigma}')\cdot\mathbf{k}'\times\delta(\mathbf{r})\mathbf{k}\,,\end{aligned} \tag{1.1}$$

where $\mathbf{r}=\mathbf{r}_1-\mathbf{r}_2$, $\mathbf{R}=(\mathbf{r}_1+\mathbf{r}_2)/2$, $\mathbf{k}=(\boldsymbol{\nabla}_1-\boldsymbol{\nabla}_2)/2i$ is the relative momentum acting on the right and $\mathbf{k}'$ is its conjugate acting on the left, $\hat{P}_\sigma=(1+\boldsymbol{\sigma}\cdot\boldsymbol{\sigma}')/2$ is the spin exchange operator and $\gamma, t_i$ and $x_i$ are the parameters of the force. The contact terms provide the S-wave contributions while momentum dependent ones (gradient terms) give the P-wave components. The

spin-orbit term ($W_0$) is irrelevant for infinite nuclear and neutron matter and we will not consider it in our calculations.

The main advantage of these forces comes from their analytical character which makes it very useful to get a physical insight into problems where the fully microscopic calculations are either very time-consuming or not yet possible to implement. Notice that not all the Skyrme parameters can be completely well determined through the fits of given sets of data and only certain combinations related to the basic properties mentioned before are really empirically determined [13].

This leads to a scenario where, for instance, different Skyrme forces produce similar EoS for symmetric nuclear matter but very different results for neutron matter. This is easily understood if one considers that neutron matter or, equivalently, systems with large isospin asymmetry are not part of the common input data employed to determine the parameters of the interaction. This feature should be corrected if Skyrme-type forces are to be used in conditions of large neutron to proton ratios such as neutron matter in neutron stars or nuclei near the drip line.

Recently, an extensive and systematic study has tested the capabilities of almost 90 existing Skyrme parametrizations to provide good neutron-star properties [14]. It was found that only 27 of these forces passed the restrictive tests imposed, the key being the behaviour (increasing) of the symmetry energy $E_{sym}(\rho)$ with density. A very convenient set of Skyrme forces are the ones provided by the Lyon group [15, 16], which also take into account variational results for neutron matter obtained with realistic interactions to fix the parameters of the force [17]. In particular, we have chosen SLy4 for our calculations. The parameters which define SLy4 are reported in table 1.1. The properties of symmetric nuclear matter provided by SLy4 are shown in table 1.3.

| | | | |
|---|---|---|---|
| $t_0 = -2488.9\,\text{MeVfm}^3$ | $t_1 = 486.8\,\text{MeVfm}^5$ | $t_2 = -546.4\,\text{MeVfm}^5$ | $t_3 = 13\,777\,\text{MeVfm}^{7/2}$ |
| $x_0 = 0.83$ | $x_1 = -0.34$ | $x_2 = -1$ | $x_3 = 1.35$ |

TABLE 1.1: Parameters of the Skyrme SLy4 interaction. Not shown parameters are zero. $\gamma = 1/6$.

## 1.2 The Gogny interaction

The Gogny interaction, proposed in 1980 by D. Gogny [10], is a well known and extensively used effective nuclear interaction. Unlike the Skyrme force, the Gogny interaction has a build-in finite-range which brings the Gogny force closer to a realistic interaction.

There are about ten available Gogny parametrizations in the literatue [18, 19, 20, 21]. However, in our calculations we will only use the original D1 force proposed by D. Gogny.

A Gogny interaction has the following structure:

$$\begin{aligned}\hat{v}_G(\mathbf{r}) = &\sum_{i=1}^{2}(W_i + B_i\hat{P}_\sigma - H_i\hat{P}_\tau - M_i\hat{P}_\sigma\hat{P}_\tau)e^{-r^2/\mu_i^2} \\ &+t_0(1+x_0\hat{P}_\sigma)\rho^\gamma\delta(\mathbf{r}) + iW_{LS}(\boldsymbol{\sigma}+\boldsymbol{\sigma'})\boldsymbol{\nabla}'\delta(\mathbf{r})\boldsymbol{\nabla}\,,\end{aligned} \tag{1.2}$$

where $\hat{P}_\sigma = (1+\boldsymbol{\sigma}\cdot\boldsymbol{\sigma'})/2$ are the spin exchange operators, $\hat{P}_\tau = (1+\boldsymbol{\tau}\cdot\boldsymbol{\tau'})/2$ are the isospin exchange operators and $\gamma, W_i, B_i, H_i, M_i, t_i, x_i$ and $\mu_i$ are the parameters of the force. Notice that $\boldsymbol{\nabla}$ acts on the right while $\boldsymbol{\nabla}'$ acts on the left.

The finite-range part is modelled by two Gaussians with two different ranges. The force also includes a variety of spin-isospin exchange terms providing a rich spin-isospin structure. The zero-range density-dependent term helps at reproducing saturation and accounts for the effects of three-body forces. As in the Skyrme case, the spin-orbit term ($W_{(LS)}$) can be dropped for infinite nuclear and neutron matter.

The parameters which define D1 are reported in table 1.2 and the properties of symmetric nuclear matter provided by D1 are shown in table 1.3.

| $i$ | $\mu_i$ | $W_i$ | $B_i$ | $H_i$ | $M_i$ |
|---|---|---|---|---|---|
| 1 | 0.7 | -402.40 | -100.00 | -496.20 | -23.56 |
| 2 | 1.2 | -21.30 | -11.77 | 37.27 | -68.81 |

TABLE 1.2: Parameters of the Gogny force D1. $t_0 = 1350\,\text{MeVfm}^4$, $x_0 = 1$ and $\gamma = 1/3$. $\mu_i$ are in fm and the other, in MeV.

| | $\rho_0[\text{fm}^{-3}]$ | $e_0(\rho_0)[\text{MeV}]$ | $e_{sym}(\rho_0)[\text{MeV}]$ | $\kappa(\rho_0)[\text{MeV}]$ |
|---|---|---|---|---|
| Skyrme SLy4 | 0.16 | -15.97 | 32.04 | 230.9 |
| Gogny D1 | 0.166 | -16.30 | 30.70 | 229.4 |

TABLE 1.3: Properties of symmetric nuclear matter provided by the Skyrme SLy4 and Gogny D1 interactions.

# Chapter 2

# Hartree-Fock Formalism

In the previous chapter, we introduced the effective forces of Skyrme and Gogny-type that we are going to employ in this master thesis. In the present chapter, we present the Hartree-Fock formalism used to calculate the nuclear matter properties far away from the conditions that have been used to define the parameters of the effective forces, i.e., mainly properties of polarized asymmetric nuclear matter. We will study polarized asymmetric nuclear matter considered as an infinite nuclear system with four different fermionic states: neutrons with spin up and spin down having densities $\rho_{n\uparrow}$ and $\rho_{n\downarrow}$, and protons with spin up and spin down with densities $\rho_{p\uparrow}$ and $\rho_{p\downarrow}$. The total density for neutrons ($\rho_n$), protons ($\rho_p$) and nucleons ($\rho$) are given by:

$$\rho_n = \rho_{n\uparrow} + \rho_{n\downarrow}\,, \qquad \rho_p = \rho_{p\uparrow} + \rho_{p\downarrow}\,, \qquad \rho = \rho_n + \rho_p\,. \tag{2.1}$$

The asymmetry ($\beta$) and spin polarization ($\Delta$) can be defined as

$$\beta = \frac{\rho_n - \rho_p}{\rho}\,, \qquad \Delta_n = \frac{\rho_{n\uparrow} - \rho_{n\downarrow}}{\rho_n}\,, \qquad \Delta_p = \frac{\rho_{p\uparrow} - \rho_{p\downarrow}}{\rho_p}\,. \tag{2.2}$$

Notice that $\beta = 0$ denotes symmetric nuclear matter and $\beta = 1$ denotes neutron matter. Notice as well that $\Delta_n = \Delta_p = 0$ stands for non-polarized matter ($\rho_{n\uparrow} = \rho_{n\downarrow}$, $\rho_{p\uparrow} = \rho_{p\downarrow}$) while $\Delta_n = \Delta_p = \pm 1$ defines totally polarized matter (all spins are aligned along the same direction) and $\Delta_n = -\Delta_p = \pm 1$ denotes anti-polarized matter (neutron spins are aligned along the same direction while proton spins are aligned along the opposite direction).

Therefore, the single-component densities as a function of the asymmetry and the polarization are given by:

$$\rho_{\tau\sigma} = \frac{\rho}{4}(1 \pm \beta)(1 \pm \Delta_\tau)\,, \tag{2.3}$$

where $(1 + \beta)$ is for neutrons, $(1 - \beta)$ is for protons, $(1 + \Delta_\tau)$ is for spin up polarization and $(1 - \Delta_\tau)$ is for spin down polarization. The third isospin component is indicated as $\tau$, and $\tau = n, p$ stands for neutron and proton, respectively, while the third component of the spin is indicated as $\sigma$, where $\sigma = \uparrow, \downarrow$ stands for spin-up and spin-down, respectively.

## 2.1 Mean field description: Hartree-Fock

We are considering a fermionic many-body system at zero temperature under a two-body force interaction. The Hamiltonian, in second quantization, reads

$$\hat{\mathcal{H}} = \hat{T} + \hat{V} = \sum_{ij} \langle i|\hat{t}|j\rangle \, a_i^\dagger a_j + \frac{1}{2}\sum_{ijkl} \langle ij|\hat{v}|kl\rangle \, a_i^\dagger a_j^\dagger a_l a_k \,, \tag{2.4}$$

where $a_i^\dagger$ and $a_j$ are the creation and annihilation single-particle operators used to describe the system.

In our case, for infinite nuclear matter, the eigenfunctions are plane waves characterized by the quantum numbers: momentum ($\mathbf{k}$), spin ($\sigma$) and isospin ($\tau$).

$$|\mathbf{k}\sigma\tau\rangle = \frac{1}{\sqrt{\Omega}} e^{i\mathbf{k}\cdot\mathbf{r}} \chi_\sigma \chi_\tau \,, \tag{2.5}$$

where $\chi_\sigma$ and $\chi_\tau$ for $\sigma, \tau = +\frac{1}{2}, -\frac{1}{2}$ are the Pauli-spinors

$$\chi_{+\frac{1}{2}} = \begin{pmatrix} 1 \\ 0 \end{pmatrix}, \qquad \chi_{-\frac{1}{2}} = \begin{pmatrix} 0 \\ 1 \end{pmatrix}, \tag{2.6}$$

respectively. The states $|\mathbf{k}\sigma\tau\rangle$ are normalized to volume:

$$\langle \mathbf{k}\sigma\tau|\mathbf{k}'\sigma'\tau'\rangle = \delta_{kk'}\delta_{\sigma\sigma'}\delta_{\tau\tau'} \,. \tag{2.7}$$

At the end of the calculations we take the thermodynamic limit, $\Omega \to \infty$ and $N \to \infty$, keeping the density defined by the ratio $N/\Omega$ constant, with $N$ being the number of particles and $\Omega$ being the volume.

The solution of the Hartree-Fock equations for an infinite system is directly provided by the plane waves. Therefore, the ground state wave function in the Hartree-Fock approximation is defined as the Slater determinant with all the single-particle levels occupied up to the Fermi level. In this case, the Hartree-Fock energy per particle coincides with the expectation value of the Hamiltonian in the free Fermi sea wave function, $\Psi_{FS}$:

$$\begin{aligned} e = \frac{E}{N} =& \frac{1}{N}\Big[ \langle \Psi_{FS}|\hat{T}|\Psi_{FS}\rangle + \langle \Psi_{FS}|\hat{V}|\Psi_{FS}\rangle \Big] \\ =& \frac{1}{N}\sum_{k\sigma\tau} \langle \mathbf{k}\sigma\tau|\hat{t}|\mathbf{k}\sigma\tau\rangle + \frac{1}{2N}\sum_{kk'\sigma\sigma'\tau\tau'} \langle \mathbf{k}\sigma\tau, \mathbf{k}'\sigma'\tau'|\hat{v}|\mathbf{k}\sigma\tau, \mathbf{k}'\sigma'\tau'\rangle_A \,. \end{aligned} \tag{2.8}$$

Notice that the kinetic energy $\langle \mathbf{k}\sigma\tau|\hat{t}|\mathbf{k}\sigma\tau\rangle = \frac{\hbar^2 k^2}{2m}$ is diagonal in this basis and the interaction energy is defined as the sum of all antisymmetrized two-body matrix elements which can be constructed with the pairs of particles.

In the Hartree-Fock approximation, the single-particle energy of a nucleon of momentum $k$ is

$$\epsilon_{\sigma\tau}(k) = \frac{\hbar^2 k^2}{2m_\tau} + U_{\sigma\tau}(k)\,, \tag{2.9}$$

where $U_{\sigma\tau}(k)$ is the single-particle potential representing the mean field felt by the nucleon of momentum $k$ with spin $\sigma$ and isospin $\tau$ due to the interaction with all the other nucleons in the system,

$$U_{\sigma\tau}(k) = \sum_{\sigma'\tau'} \sum_{k' \leq k'_{F\sigma'\tau'}} \langle \mathbf{k}\sigma\tau, \mathbf{k}'\sigma'\tau' | \hat{v} | \mathbf{k}\sigma\tau, \mathbf{k}'\sigma'\tau' \rangle_A \,, \tag{2.10}$$

being $k'_{F\sigma'\tau'}$ the Fermi momentum of each nucleon species. Notice that the antisymmetrized two-body matrix elements can be defined in the following way:

$$\langle \mathbf{k}\sigma\tau, \mathbf{k}'\sigma'\tau' | \hat{v} | \mathbf{k}\sigma\tau, \mathbf{k}'\sigma'\tau' \rangle_A = \langle \mathbf{k}\sigma\tau, \mathbf{k}'\sigma'\tau' | \hat{v}\hat{\mathcal{A}} | \mathbf{k}\sigma\tau, \mathbf{k}'\sigma'\tau' \rangle \tag{2.11}$$

where $\hat{\mathcal{A}} = (1 - \hat{P}_r \hat{P}_\sigma \hat{P}_\tau)$ is the antisymmetry operator and $\hat{P}_r$, $\hat{P}_\sigma$ and $\hat{P}_\tau$ are the position, spin and isospin exchange operators, respectively,

$$\hat{P}_\sigma \left|\sigma\sigma'\right\rangle = \left|\sigma'\sigma\right\rangle \,, \qquad \hat{P}_\tau \left|\tau\tau'\right\rangle = \left|\tau'\tau\right\rangle \,. \tag{2.12}$$

Instead of working with the third component of the spin and the isospin, we can also characterize the two-body states by the total spin $S$ and isospin $T$ and their third components $M_S$ and $M_T$. At the same time, we also use the center of mass system by defining $\mathbf{K}_{CM} = (\mathbf{k} + \mathbf{k}')/2$ and the relative momentum $\mathbf{k}_r = \mathbf{k} - \mathbf{k}'$. Then, $\hat{P}_r$, $\hat{P}_\sigma$ and $\hat{P}_\tau$ operators act as follows:

$$\begin{aligned} \hat{P}_r \left|\mathbf{K}_{CM}, \mathbf{k}_r\right\rangle &= \left|\mathbf{K}_{CM}, -\mathbf{k}_r\right\rangle \,, \\ \hat{P}_\sigma \left|SM_S\right\rangle &= (-1)^{S+1} \left|SM_S\right\rangle \,, \\ \hat{P}_\tau \left|TM_T\right\rangle &= (-1)^{T+1} \left|TM_T\right\rangle \,. \end{aligned} \tag{2.13}$$

Before going into the calculation of the energy contributions, let us compute the number of particles, given by:

$$N = \sum_{\sigma\tau} \sum_{k \leq k_{F\sigma\tau}} 1 = \sum_{\sigma\tau} \frac{\Omega}{(2\pi)^3} \int \mathrm{d}^3k\, \theta(k_{F\sigma\tau} - k) = \sum_{\sigma\tau} \frac{\Omega {k_{F\sigma\tau}}^3}{6\pi^2} \,, \tag{2.14}$$

where we took the prescription

$$\sum_k \longrightarrow \frac{\Omega}{(2\pi^3)} \int \mathrm{d}^3k \tag{2.15}$$

in order to perform the sum over momentum. Now, we can relate the Fermi momentum and the density of each species.

$$\rho_{\sigma\tau} = \frac{{k_{F\sigma\tau}}^3}{6\pi^2}\,, \qquad k_{F\sigma\tau} = \left(6\pi^2\rho_{\sigma\tau}\right)^{1/3}. \tag{2.16}$$

Notice that in the Hartree-Fock approximation only the diagonal matrix elements are used.

## 2.2 Two-body matrix elements

In the next step we should calculate the antisymmetrized two-body matrix elements which we decomposed in a direct and an exchange term:

- Direct term:

$$\begin{aligned}
&\langle \mathbf{k}\sigma\tau, \mathbf{k}'\sigma'\tau'|\hat{v}|\mathbf{k}\sigma\tau, \mathbf{k}'\sigma'\tau'\rangle = \\
&= \int\int \mathrm{d}^3r_1\,\mathrm{d}^3r_2\,\frac{1}{\sqrt{\Omega}}e^{-i\mathbf{k}\cdot\mathbf{r_1}}\frac{1}{\sqrt{\Omega}}e^{-i\mathbf{k}'\cdot\mathbf{r_2}}\hat{v}(\mathbf{r}_1-\mathbf{r}_2) \\
&\qquad \times \frac{1}{\sqrt{\Omega}}e^{i\mathbf{k}\cdot\mathbf{r_1}}\frac{1}{\sqrt{\Omega}}e^{i\mathbf{k}'\cdot\mathbf{r_2}}\,\langle\sigma\sigma'|\hat{O}_\sigma|\sigma\sigma'\rangle\,\langle\tau\tau'|\hat{O}_\tau|\tau\tau'\rangle \\
&= \frac{1}{\Omega^2}\int\int \mathrm{d}^3r_1\,\mathrm{d}^3r_2\,\hat{v}(\mathbf{r}_1-\mathbf{r}_2)\,\langle\sigma\sigma'|\hat{O}_\sigma|\sigma\sigma'\rangle\,\langle\tau\tau'|\hat{O}_\tau|\tau\tau'\rangle\,.
\end{aligned} \tag{2.17}$$

- Exchange term:

$$\begin{aligned}
&\langle \mathbf{k}\sigma\tau, \mathbf{k}'\sigma'\tau'|\hat{v}|\mathbf{k}'\sigma'\tau', \mathbf{k}\sigma\tau\rangle = \\
&= \int\int \mathrm{d}^3r_1\,\mathrm{d}^3r_2\,\frac{1}{\sqrt{\Omega}}e^{-i\mathbf{k}\cdot\mathbf{r_1}}\frac{1}{\sqrt{\Omega}}e^{-i\mathbf{k}'\cdot\mathbf{r_2}}\hat{v}(\mathbf{r}_1-\mathbf{r}_2) \\
&\qquad \times \frac{1}{\sqrt{\Omega}}e^{i\mathbf{k}'\cdot\mathbf{r_1}}\frac{1}{\sqrt{\Omega}}e^{i\mathbf{k}\cdot\mathbf{r_2}}\,\langle\sigma\sigma'|\hat{O}_\sigma|\sigma'\sigma\rangle\,\langle\tau\tau'|\hat{O}_\tau|\tau'\tau\rangle \\
&= \frac{1}{\Omega^2}\int\int \mathrm{d}^3r_1\,\mathrm{d}^3r_2\,\hat{v}(\mathbf{r}_1-\mathbf{r}_2)e^{-i\mathbf{k}\cdot(\mathbf{r_1}-\mathbf{r_2})}e^{i\mathbf{k}'\cdot(\mathbf{r_1}-\mathbf{r_2})}\,\langle\sigma\sigma'|\hat{O}_\sigma|\sigma'\sigma\rangle\,\langle\tau\tau'|\hat{O}_\tau|\tau'\tau\rangle\,.
\end{aligned} \tag{2.18}$$

In the case of the Skyrme interaction, the antisymmetrized two-body matrix elements can be written as

$$\begin{aligned}\langle \mathbf{k}\sigma\tau, \mathbf{k}'\sigma'\tau'|\hat{v}_{Sk}(\mathbf{r})|\mathbf{k}\sigma\tau, \mathbf{k}'\sigma'\tau'\rangle_A = \\ = \frac{1}{\Omega}\Bigg[t_0 + \frac{1}{6}t_3\rho^\gamma + \frac{1}{4}(\mathbf{k}-\mathbf{k}')^2(t_1+t_2) \\ + \left\{t_0x_0 + \frac{1}{6}t_3x_3\rho^\gamma + \frac{1}{4}(\mathbf{k}-\mathbf{k}')^2(t_1x_1+t_2x_2)\right\}\delta_{\sigma\sigma'} \\ - \left\{t_0 + \frac{1}{6}t_3\rho^\gamma + \frac{1}{4}(\mathbf{k}-\mathbf{k}')^2(t_1-t_2)\right\}\delta_{\sigma\sigma'}\delta_{\tau\tau'} \\ - \left\{t_0x_0 + \frac{1}{6}t_3x_3\rho^\gamma + \frac{1}{4}(\mathbf{k}-\mathbf{k}')^2(t_1x_1-t_2x_2)\right\}\delta_{\tau\tau'}\Bigg],\end{aligned} \tag{2.19}$$

while for the Gogny interaction we have

$$\begin{aligned}\langle k_1s_1\tau_1, k_2s_2\tau_2|\hat{v}_G(\mathbf{r})|k_1s_1\tau_1, k_2s_2\tau_2\rangle_A = \\ = \frac{1}{\Omega}\rho^\gamma t_0[(1-\delta_{s_1s_2}\delta_{\tau_1\tau_2}) + x_0(\delta_{s_1s_2}-\delta_{\tau_1\tau_2})] \\ + \frac{1}{\Omega}\pi^{3/2}\sum_i \mu_i^3 \\ \times \Bigg[W_i\left(1-\delta_{s_1s_2}\delta_{\tau_1\tau_2}e^{-\frac{\mu_i^2}{4}|\mathbf{q}|^2}\right) + B_i\left(\delta_{s_1s_2}-\delta_{\tau_1\tau_2}e^{-\frac{\mu_i^2}{4}|\mathbf{q}|^2}\right) \\ - H_i\left(\delta_{\tau_1\tau_2}-\delta_{s_1s_2}e^{-\frac{\mu_i^2}{4}|\mathbf{q}|^2}\right) - M_i\left(\delta_{s_1s_2}\delta_{\tau_1\tau_2}-e^{-\frac{\mu_i^2}{4}|\mathbf{q}|^2}\right)\Bigg],\end{aligned} \tag{2.20}$$

where $\mathbf{q} = \mathbf{k} - \mathbf{k}'$.

In Fig. 2.1 we present the matrix elements of the Skyrme SLy4 (letf) and Gogny D1 (right) interactions times volume as functions of the momentum $k'$ at saturation density $\rho_0 = 0.16\,\mathrm{fm}^{-3}$ with $k = 0\,\mathrm{fm}^{-1}$. Notice that Eqs. (2.19) and (2.20) are symmetric under the exchange of $k$ and $k'$.

The Skyrme SLy4 diagonal matrix elements where nucleons have the same third spin component ($\sigma = \sigma'$) and the same isospin third component ($\tau = \tau'$) are set to zero in the SLy4 parametrization. Otherwise, all the Gogny D1 matrix elements are different than zero, although the ones with the same third spin and isospin component are almost null.

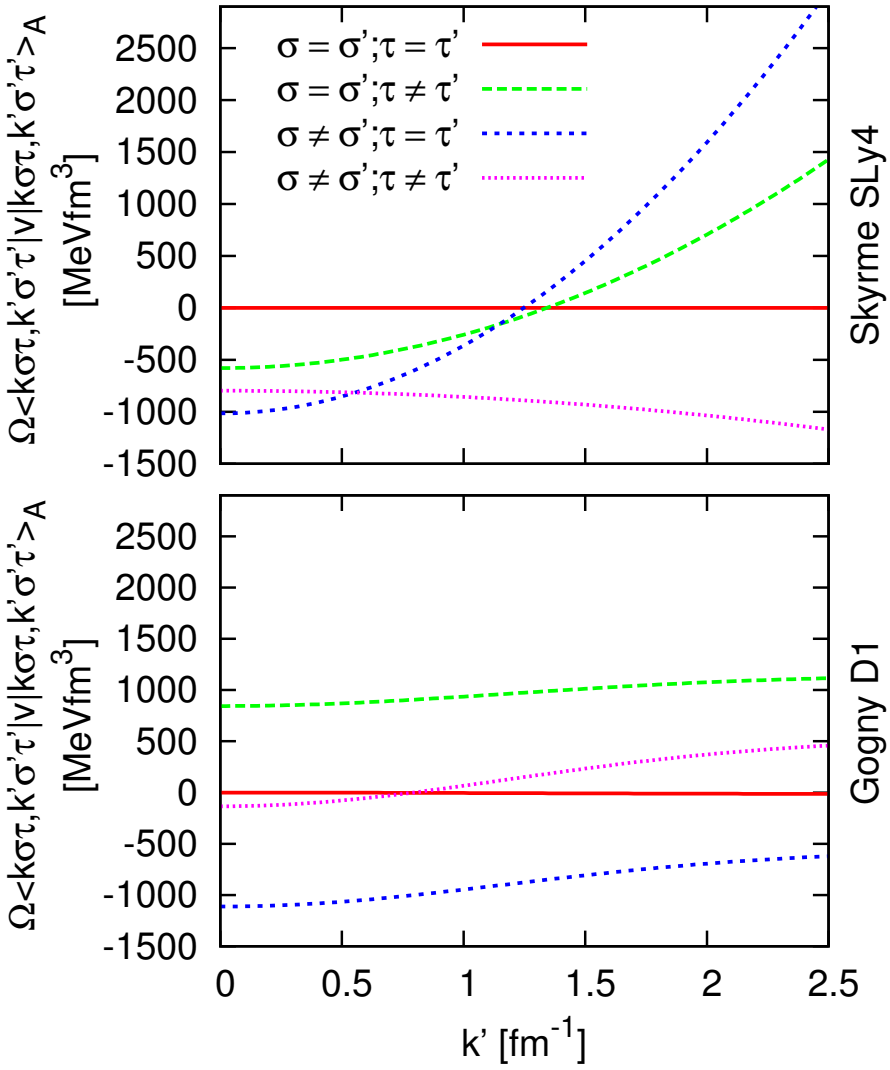


FIGURE 2.1: Matrix elements of the Skyrme SLy4 (top) and Gogny D1 (bottom) interactions times volume as functions of the momentum $k'$ at saturation density $\rho_0 = 0.16\,\mathrm{fm}^{-3}$ with $k = 0\,\mathrm{fm}^{-1}$.

# Chapter 3

# Energy Contributions

After presenting the two families of effective forces (Skyrme and Gogny) considered in Chapter 1, and with the framework developed in Chapter 2, in this chapter we present the calculations of the total energy of polarized asymmetric nuclear matter and the single-particle potential that feels a nucleon with momentum $k$ and a given third component of the spin ($\sigma$) and isospin ($\tau$) due to the interaction with the other nucleons.

We calculate first the single-particle potential followed by the calculation of the kinetic and potential energies, which define the total energy of the system. The calculation of the potential energy is performed by summing all the two-body matrix elements. After that, we present an alternative calculation for the potential energy using the Slater functions, which is equivalent to the calculation of the distribution function of the free Fermi sea. Finally, we calculate the isospin and spin symmetry energies.

## 3.1 Single-Particle Potential

The single-particle potential, defined in Eq. (2.10), is

$$U_{\sigma\tau}(k) = \sum_{\sigma'\tau'} \sum_{k' \leq k'_{F\sigma'\tau'}} \langle \mathbf{k}\sigma\tau, \mathbf{k}'\sigma'\tau' | \hat{v} | \mathbf{k}\sigma\tau, \mathbf{k}'\sigma'\tau' \rangle_A \ . \tag{3.1}$$

In the case of the Skyrme interaction, the single-particle potential for a given $\sigma$ and $\tau$, calculated using Eq. (2.19) and Eq. (3.1), has the following expression:

$$\begin{aligned} U^{\mathrm{Sk}}_{\sigma\tau}(k) = \sum_{\sigma'\tau'} \Bigg\{ & \left[ t_0 + \frac{1}{6} t_3 \rho^\gamma + \frac{1}{4} \left( k^2 + \frac{3}{5} {k'_{F\sigma'\tau'}}^2 \right) (t_1 + t_2) \right] \rho_{\sigma'\tau'} \\ & + \left[ t_0 x_0 + \frac{1}{6} t_3 x_3 \rho^\gamma + \frac{1}{4} \left( k^2 + \frac{3}{5} {k'_{F\sigma'\tau'}}^2 \right) (t_1 x_1 + t_2 x_2) \right] \rho_{\sigma'\tau'} \delta_{\sigma\sigma'} \\ & - \left[ t_0 + \frac{1}{6} t_3 \rho^\gamma + \frac{1}{4} \left( k^2 + \frac{3}{5} {k'_{F\sigma'\tau'}}^2 \right) (t_1 - t_2) \right] \rho_{\sigma'\tau'} \delta_{\sigma\sigma'} \delta_{\tau\tau'} \\ & - \left[ t_0 x_0 + \frac{1}{6} t_3 x_3 \rho^\gamma + \frac{1}{4} \left( k^2 + \frac{3}{5} {k'_{F\sigma'\tau'}}^2 \right) (t_1 x_1 - t_2 x_2) \right] \rho_{\sigma'\tau'} \delta_{\tau\tau'} \Bigg\} , \end{aligned} \tag{3.2}$$

being $k'_{F\sigma'\tau'}$ the Fermi momentum for the $\sigma'\tau'$ component, Eq. (2.16). Notice that the single-particle spectrum is parabolic in $k$ and, therefore, the effective mass is momentum independent.

For the Gogny force, the single-particle potential for a given $\sigma\tau$, calculated using Eq. (2.20) and Eq. (3.1), reads

$$\begin{aligned} U^{\mathrm{G}}_{\sigma\tau}(k) = \sum_{\sigma'\tau'} \Bigg\{ & \rho^{\gamma} t_0 [(1 - \delta_{\sigma\sigma'}\delta_{\tau\tau'}) + x_0(\delta_{\sigma\sigma'} - \delta\tau\tau')]\rho_{\sigma'\tau'} \\ & + \pi^{3/2} \sum_i \mu_i^3 [W_i + B_i\delta_{\sigma\sigma'} - H_i\delta_{\tau\tau'} - M_i\delta_{\sigma\sigma'}\delta\tau\tau']\rho_{\sigma'\tau'} \\ & - \frac{1}{\sqrt{\pi}} \sum_i [W_i\delta_{\sigma\sigma'}\delta_{\tau\tau'} + B_i\delta_{\tau\tau'} - H_i\delta_{\sigma\sigma'} - M_i] \\ & \times \left[ \frac{1}{\mu_i k} \left( e^{-q_+^2} - e^{-q_-^2} \right) + \frac{\sqrt{\pi}}{2} \operatorname{erf}(q_-, q_+) \right] \Bigg\}, \end{aligned} \tag{3.3}$$

where $q_\pm = \frac{\mu_i}{2}(k \pm k'_{F\sigma'\tau'})$ and $\operatorname{erf}(a,b) = \frac{2}{\sqrt{\pi}} \int_a^b \mathrm{d}x\, e^{-x^2}$ is the error function. Notice that the last term of the previous equation should be carefully computed when $k = 0$. In this case $U^{\mathrm{G}}_{\sigma\tau}(k=0)$ reads

$$\begin{aligned} U^{\mathrm{G}}_{\sigma\tau}(0) = \sum_{\sigma'\tau'} \Bigg\{ & \rho^{\gamma} t_0 [(1 - \delta_{\sigma\sigma'}\delta_{\tau\tau'}) + x_0(\delta_{\sigma\sigma'} - \delta\tau\tau')]\rho_{\sigma'\tau'} \\ & + \pi^{3/2} \sum_i \mu_i^3 [W_i + B_i\delta_{\sigma\sigma'} - H_i\delta_{\tau\tau'} - M_i\delta_{\sigma\sigma'}\delta\tau\tau']\rho_{\sigma'\tau'} \\ & - \frac{1}{\sqrt{\pi}} \sum_i [W_i\delta_{\sigma\sigma'}\delta_{\tau\tau'} + B_i\delta_{\tau\tau'} - H_i\delta_{\sigma\sigma'} - M_i] \\ & \times \left[ \sqrt{\pi} \operatorname{erf}\left( \frac{\mu_i k'_{F\sigma'\tau'}}{2} \right) - \mu_i k'_{F\sigma'\tau'} e^{-\frac{\mu_i^2}{4} {k'_{F\sigma'\tau'}}^2} \right] \Bigg\}. \end{aligned} \tag{3.4}$$

In Figs. 3.1 and 3.2, we show the results of the single-particle potential for the Skyrme SLy4 interaction and the Gogny D1 interaction, respectively. Both figures show the neutron ($U_{n\uparrow}(k)$ , $U_{n\downarrow}(k)$) (upper panels) and proton ($U_{p\uparrow}(k)$, $U_{p\downarrow}(k)$) single-particle potentials for different asymmetries ($\beta$) and spin polarizations ($\Delta_n, \Delta_p$) at saturation density $\rho_0 = 0.16\,\mathrm{fm}^{-3}$. The results for symmetric nuclear matter ($\beta = 0$) are shown in the left and central columns, whereas the results for asymmetric nuclear matter with $\beta = 0.5$ are shown in the right column. Solid black lines show the results of non-polarized matter ($\Delta_n = \Delta_p = 0$) as a reference. Dotted red and green lines show the results of spin-polarized matter.

The main difference between the Skyrme SLy4 and the Gogny D1 interactions is that the single-particle potential for the Skyrme SLy4 interaction shows a parabolic behaviour with $k$, see Eq. (3.2), whereas the single-particle potential for the Gogny D1 interaction does not show a global parabolic behaviour in the full range of $k$, see Eq. (3.3), showing a saturation behaviour for large values of $k$. This effect is caused because the Skyrme interaction is a

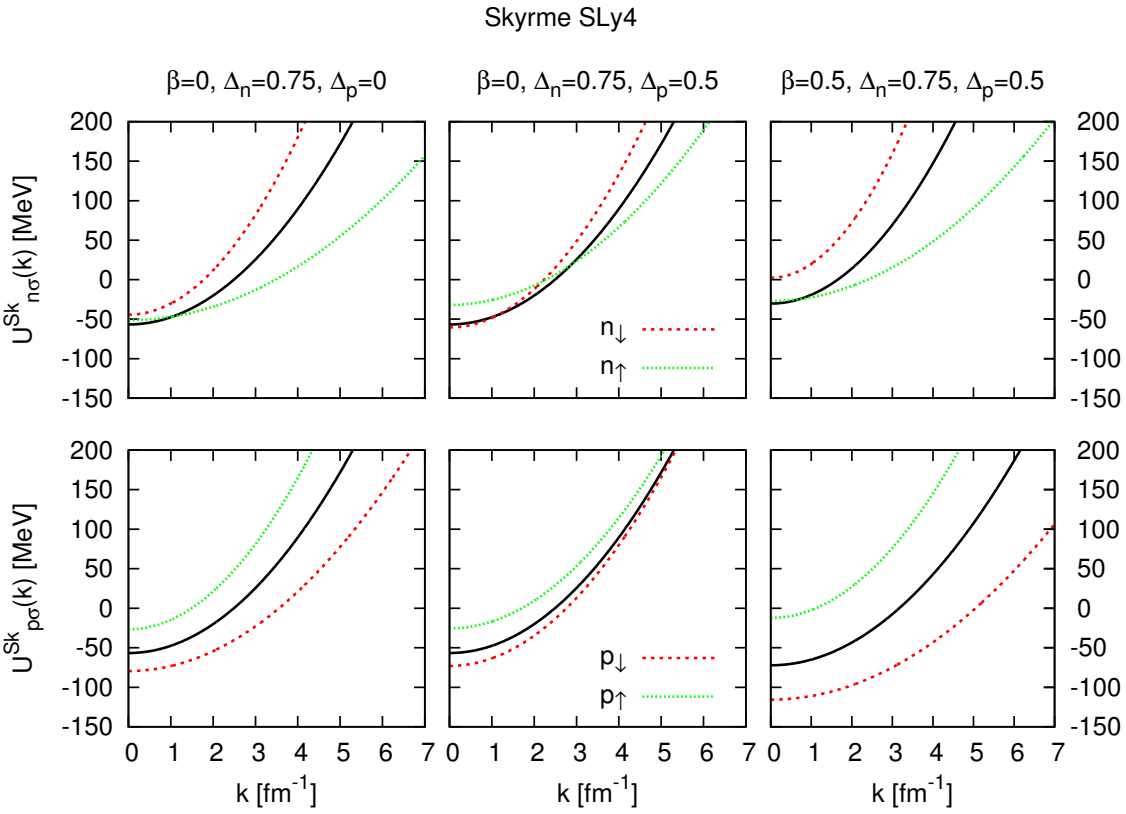


FIGURE 3.1: Skyrme SLy4 interaction single-particle potentials. Upper panels show the neutron single-particle potentials and lower panels show the proton single-particle potentials as a function of momentum $k$ for different asymmetries and spin polarizations at saturation density of symmetric nuclear matter $\rho_0 = 0.16\,\mathrm{fm}^{-3}$. Left and central panels show results for symmetric nuclear matter whereas right panels shows results for asymmetric matter. Solid black lines show the results for non-polarized matter ($\Delta_n = \Delta_p = 0$) as a reference, whereas dotted red and green lines show the results for spin-polarized matter.

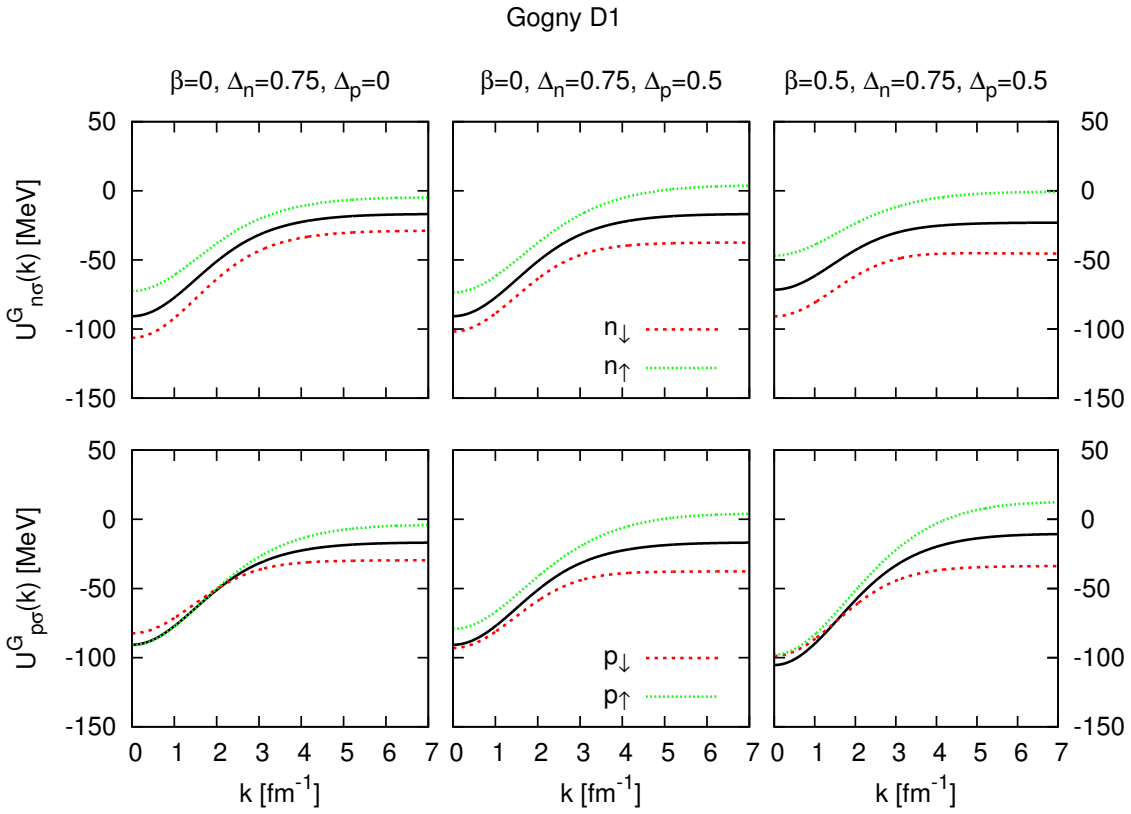


FIGURE 3.2: Gogny D1 interaction single-particle potentials. Upper panels show the neutron single-particle potentials and lower panels show the proton single-particle potentials as a function of momentum $k$ for different asymmetries and spin polarizations at saturation density of symmetric nuclear matter $\rho_0 = 0.16\,\mathrm{fm}^{-3}$. Left and central panels show results for symmetric nuclear matter whereas right panels shows results for asymmetric matter. Solid black lines show the results for non-polarized matter ($\Delta_n = \Delta_p = 0$) as a reference, whereas dotted red and green lines show the results for spin-polarized matter.

zero-range force while the Gogny interaction has a finite-range. Notice that the saturation behaviour of the single-particle potential for the Gogny interaction for large $k$ is a consequence of the fact that the exchange term of the interaction goes to zero. Thus, the contribution for large $k$ is provided by the direct term, which has no momentum dependence.

One can point out that for non-polarized asymmetric nuclear matter the single-particle spectrum for protons becomes more attractive than the one for neutrons. This is true for both the Skyrme SLy4 and the Gogny D1 interactions. It can be seen by comparing the solid black lines of the upper and lower right column panels of both previous figures.

Concerning the dependence of the single-particle potentials of the species with the spin-polarization, we observe an opposite behaviour for the polarized neutrons. In fact, the single-particle potential of the less abundant component ($n\downarrow$) becomes more attractive than that of the most abundant component ($n\uparrow$) in the case of the Gogny D1 interaction. The opposite is true for the Skyrme SLy4 interaction. For the proton single-particle spectrum, we observe a similar behaviour for both forces, being, in general, the less abundant component ($p\downarrow$) more attractive, for both interactions.

## 3.2 Kinetic and Potential Energies

We have already calculated the single-particle spectrum of the different species for different spin polarizations and isospin asymmetries. The next step will be to calculate the kinetic and the potential energy contributions to the total energy.

The kinetic energy per particle[1], in a fermionic system composed by different species, is the following:

$$\begin{aligned}\frac{1}{N}\langle\Psi|\hat{T}|\Psi\rangle = \frac{1}{N}\sum_{\sigma\tau}\sum_{k<k_{F\sigma\tau}}\langle\mathbf{k}\sigma\tau|\hat{k}|\mathbf{k}\sigma\tau\rangle &= \frac{3}{5}\frac{\hbar^2}{2m_n}(k_{Fn\uparrow}^2+k_{Fn\downarrow}^2)+\frac{3}{5}\frac{\hbar^2}{2m_p}(k_{Fp\uparrow}^2+k_{Fp\downarrow}^2)\\ &= \frac{\hbar^2}{2m_n}\frac{1}{\rho}(\xi_{n\uparrow}+\xi_{n\downarrow})+\frac{\hbar^2}{2m_p}\frac{1}{\rho}(\xi_{p\uparrow}+\xi_{p\downarrow})\,,\end{aligned} \tag{3.5}$$

where $\xi_{\tau\sigma}$ are related to the average kinetic energy of the Fermi model of nuclear matter [22],

$$\begin{aligned}\xi_{\tau\sigma} &= \frac{3}{5}k_{F\sigma\tau}^2\rho_{\tau\sigma} = \frac{3}{5}(6\pi^2\rho_{\tau\sigma})^{2/3}\rho_{\tau\sigma}\\ &= \frac{3}{20}\left(\frac{3}{2}\pi^2\rho\right)^{2/3}\rho(1\pm\beta)^{5/3}(1\pm\Delta_\tau)^{5/3}\,.\end{aligned} \tag{3.6}$$

[1]The kinetic energy per particle as a function of the total density $\rho$, isospin asymmetry $\beta$ and neutron and proton spin polarizations $\Delta_n$ and $\Delta_p$ is provided by Eq. (A.10)

The potential energy per particle can be calculated by performing the sum over the spin and isospin components and the momentum $k$ up to the Fermi momentum $k_{F\sigma\tau}$ of the single-particle potential of nucleons with momentum $k$ spin $\sigma$ and isospin $\tau$:

$$\frac{1}{N}\langle\Psi_{FS}|\hat{V}|\Psi_{FS}\rangle = \frac{1}{2N}\sum_{\sigma\tau}\sum_{k\leq k_{F\sigma\tau}} U_{\sigma\tau}(k)\,. \tag{3.7}$$

Equivalently, using Eq.(3.1), the previous expression can be written as

$$\frac{\langle V\rangle}{N} = \frac{1}{2N}\sum_{\sigma\sigma'\tau\tau'}\frac{\Omega^2}{(2\pi)^6}\int_{k_{F\sigma\tau}}\int_{k'_{F\sigma'\tau'}} \mathrm{d}^3\mathbf{k}\,\mathrm{d}^3\mathbf{k}'\ \langle\mathbf{k}\sigma\tau,\mathbf{k}'\sigma'\tau'|\hat{v}|\mathbf{k}\sigma\tau,\mathbf{k}'\sigma'\tau'\rangle_A\ , \tag{3.8}$$

where the integrals over momentum can be expressed in terms of a function $\Phi(\mathbf{k},\mathbf{k}')$ with a $k,k'$ dependence, can be found in the appendix A.1 for both the Skyrme and Gogny interactions.

$$I[\Phi(\mathbf{k},\mathbf{k}');k_{F\sigma\tau},k'_{F\sigma'\tau'}] \equiv \frac{1}{2N}\frac{\Omega^2}{(2\pi)^6}\int_{k_{F\sigma\tau}}\int_{k'_{F\sigma'\tau'}} \mathrm{d}^3\mathbf{k}\,\mathrm{d}^3\mathbf{k}'\,\Phi(\mathbf{k},\mathbf{k}')\,. \tag{3.9}$$

For the Skyrme interaction, the potential energy per particle[2] reads

$$\begin{aligned}
\frac{\langle V^{\mathrm{Sk}}\rangle}{N} &= \frac{1}{4\rho}[2t_2(1+x_2)][\xi_{n\uparrow}\rho_{n\uparrow}+\xi_{n\downarrow}\rho_{n\downarrow}+\xi_{p\uparrow}\rho_{p\uparrow}+\xi_{p\downarrow}\rho_{p\downarrow}]\\
&+\frac{1}{4\rho}[t_1(1-x_1)+t_2(1+x_2)][\xi_{n\uparrow}\rho_{n\downarrow}+\xi_{n\downarrow}\rho_{n\uparrow}+\xi_{p\uparrow}\rho_{p\downarrow}+\xi_{p\downarrow}\rho_{p\uparrow}]\\
&+\frac{1}{4\rho}[t_1(1+x_1)+t_2(1+x_2)][\xi_{n\uparrow}\rho_{p\uparrow}+\xi_{n\downarrow}\rho_{p\downarrow}+\xi_{p\uparrow}\rho_{n\uparrow}+\xi_{p\downarrow}\rho_{n\downarrow}]\\
&+\frac{1}{4\rho}[t_1+t_2][\xi_{n\uparrow}\rho_{p\downarrow}+\xi_{n\downarrow}\rho_{p\uparrow}+\xi_{p\uparrow}\rho_{n\downarrow}+\xi_{p\downarrow}\rho_{n\uparrow}]\\
&+\frac{1}{\rho}\left[t_0+\frac{1}{6}t_3\rho^\gamma\right]\rho_n\rho_p+\frac{1}{\rho}\left[t_0x_0+\frac{1}{6}t_3x_3\rho^\gamma\right][\rho_{n\uparrow}\rho_{p\uparrow}+\rho_{n\downarrow}\rho_{p\downarrow}]\\
&+\frac{1}{\rho}\left[t_0(1-x_0)+\frac{1}{6}t_3(1-x_3)\rho^\gamma\right][\rho_{n\uparrow}\rho_{n\downarrow}+\rho_{p\uparrow}\rho_{p\downarrow}]\,,
\end{aligned} \tag{3.10}$$

[2]The Skyrme potential energy per particle as a function of the total density $\rho$, isospin asymmetry $\beta$ and neutron and proton spin polarizations $\Delta_n$ and $\Delta_p$ is provided by Eq. (A.11)

while the potential energy per particle for the Gogny interaction reads

$$\begin{aligned}
\frac{\langle V^{\rm G}\rangle}{N} &= \rho^{\gamma-1}t_0(1-x_0)(\rho_{n\uparrow}\rho_{n\downarrow}+\rho_{p\uparrow}\rho_{p\downarrow})+\rho^{\gamma-1}t_0\rho_n\rho_p+\rho^{\gamma-1}t_0x_0(\rho_{n\uparrow}\rho_{p\uparrow}+\rho_{n\downarrow}\rho_{p\downarrow})\\
&+\frac{\pi^{3/2}}{2\rho}\sum_i\mu_i^3\Big[W_i\rho^2+B_i\big[(\rho_{n\uparrow}+\rho_{p\uparrow})^2+(\rho_{n\downarrow}+\rho_{p\downarrow})^2\big]\\
&\qquad -H_i(\rho_n^2+\rho_p^2)-M_i(\rho_{n\uparrow}^2+\rho_{n\downarrow}^2+\rho_{p\uparrow}^2+\rho_{p\downarrow}^2)\Big]\\
&-\frac{1}{4\rho\sqrt{\pi}}\sum_i\Big[(W_i+B_i-H_i-M_i)\Big(g_i(k_{Fn\uparrow},k_{Fn\uparrow})+g_i(k_{Fn\downarrow},k_{Fn\downarrow})\\
&\qquad +g_i(k_{Fp\uparrow},k_{Fp\uparrow})+g_i(k_{Fp\downarrow},k_{Fp\downarrow})\Big)\\
&\qquad +(B_i-M_i)\Big(g_i(k_{Fn\uparrow},k_{Fn\downarrow})+g_i(k_{Fn\downarrow},k_{Fn\uparrow})\\
&\qquad +g_i(k_{Fp\uparrow},k_{Fp\downarrow})+g_i(k_{Fp\downarrow},k_{Fp\uparrow})\Big)\\
&\qquad -(H_i+M_i)\Big(g_i(k_{Fn\uparrow},k_{Fp\uparrow})+g_i(k_{Fn\downarrow},k_{Fp\downarrow})\\
&\qquad +g_i(k_{Fp\uparrow},k_{Fn\uparrow})+g_i(k_{Fp\downarrow},k_{Fn\downarrow})\Big)\\
&\qquad -M_i\Big(g_i(k_{Fn\uparrow},k_{Fp\downarrow})+g_i(k_{Fn\downarrow},k_{Fp\uparrow})\\
&\qquad +g_i(k_{Fp\uparrow},k_{Fn\downarrow})+g_i(k_{Fp\downarrow},k_{Fn\uparrow})\Big)\Big],
\end{aligned}\tag{3.11}$$

where

$$\begin{aligned}
g_i(k_{F\sigma\tau},k'_{F\sigma'\tau'}) &= \frac{1}{3\pi^2\mu_i^3}\Big[\big(\mu_i^2k_{F\sigma\tau}^2-\mu_ik_{F\sigma\tau}\mu_ik'_{F\sigma'\tau'}+\mu_i^2k'^2_{F\sigma'\tau'}-2\big)e^{-\frac{\mu_i^2}{4}(k_{F\sigma\tau}+k'_{F\sigma'\tau'})^2}\\
&-\big(\mu_i^2k_{F\sigma\tau}^2+\mu_ik_{F\sigma\tau}\mu_ik'_{F\sigma'\tau'}+\mu_i^2k'^2_{F\sigma'\tau'}-2\big)e^{-\frac{\mu_i^2}{4}(k_{F\sigma\tau}-k'_{F\sigma'\tau'})^2}\\
&-\frac{\sqrt{\pi}\mu_i^3}{2}\big(k_{F\sigma\tau}^3-k'^3_{F\sigma'\tau'}\big)\,\mathrm{erf}\left(\frac{\mu_i}{2}(k_{F\sigma\tau}-k'_{F\sigma'\tau'})\right)\\
&+\frac{\sqrt{\pi}\mu_i^3}{2}\big(k_{F\sigma\tau}^3+k'^3_{F\sigma'\tau'}\big)\,\mathrm{erf}\left(\frac{\mu_i}{2}(k_{F\sigma\tau}+k'_{F\sigma'\tau'})\right)\Big].
\end{aligned}\tag{3.12}$$

Notice that $g_i(k_{F\sigma\tau},0)=g_i(0,k'_{F\sigma'\tau'})=g_i(0,0)=0$.

In Fig. 3.3 we show the kinetic energy (upper row) and the potential energy per particle for the Skyrme SLy4 interaction (middle row) and for the Gogny D1 interaction (lower row) for non-polarized ($\Delta_n=\Delta_p=0$), totally polarized ($\Delta_n=\Delta_p=\pm1$) and anti-polarized ($\Delta_n=-\Delta_p=\pm1$) nuclear matter. The case of symmetric nuclear matter ($\beta=0$) is shown in the left column, asymmetric nuclear matter with $\beta=0.5$ is shown in the central column and neutron matter ($\beta=1$) is presented in the right column.

First of all, we observe that the kinetic energy increases with the isospin

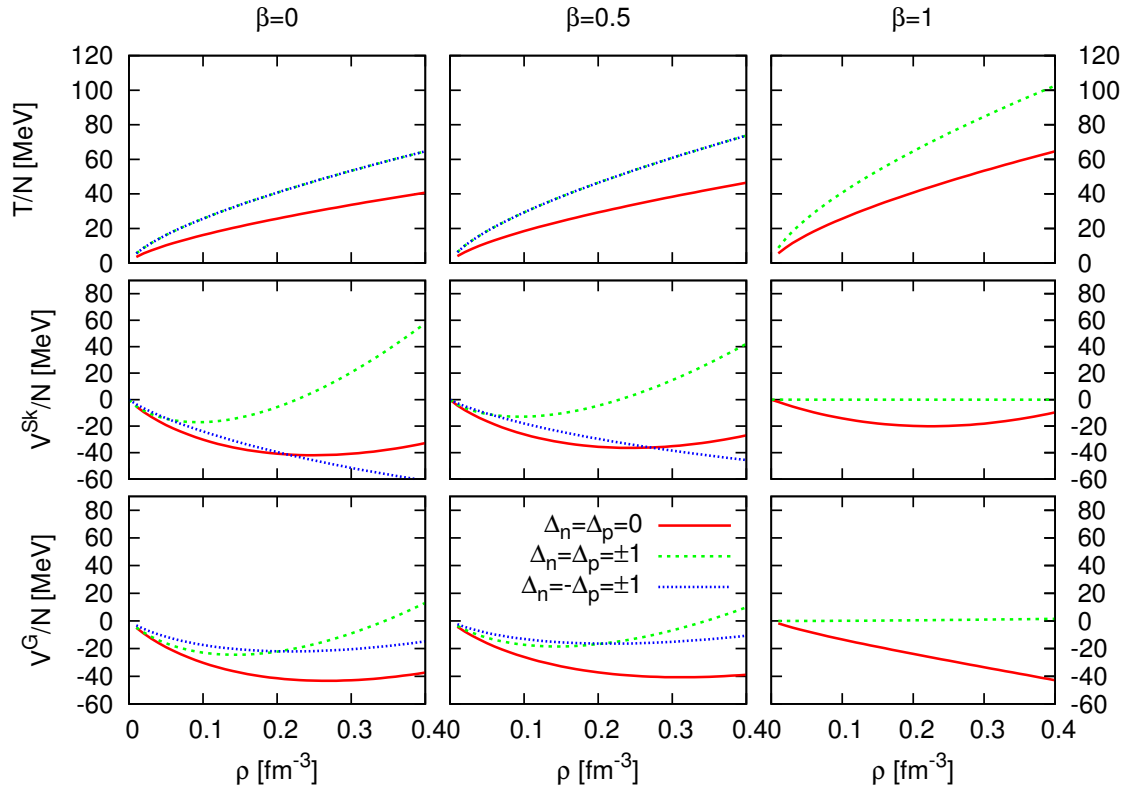


FIGURE 3.3: Kinetic (upper row) and potential (middle and lower row) energy per particle for the Skyrme SLy4 interaction (middle row) and for the Gogny D1 interaction (lower row) as functions of the total density for symmetric nuclear matter (left column), asymmetric nuclear matter (central column) and neutron matter (right column) and non-polarized ($\Delta_n = \Delta_p = 0$), totally polarized ($\Delta_n = \Delta_p = \pm 1$) and anti-polarized ($\Delta_n = -\Delta_p = \pm 1$) nuclear matter.

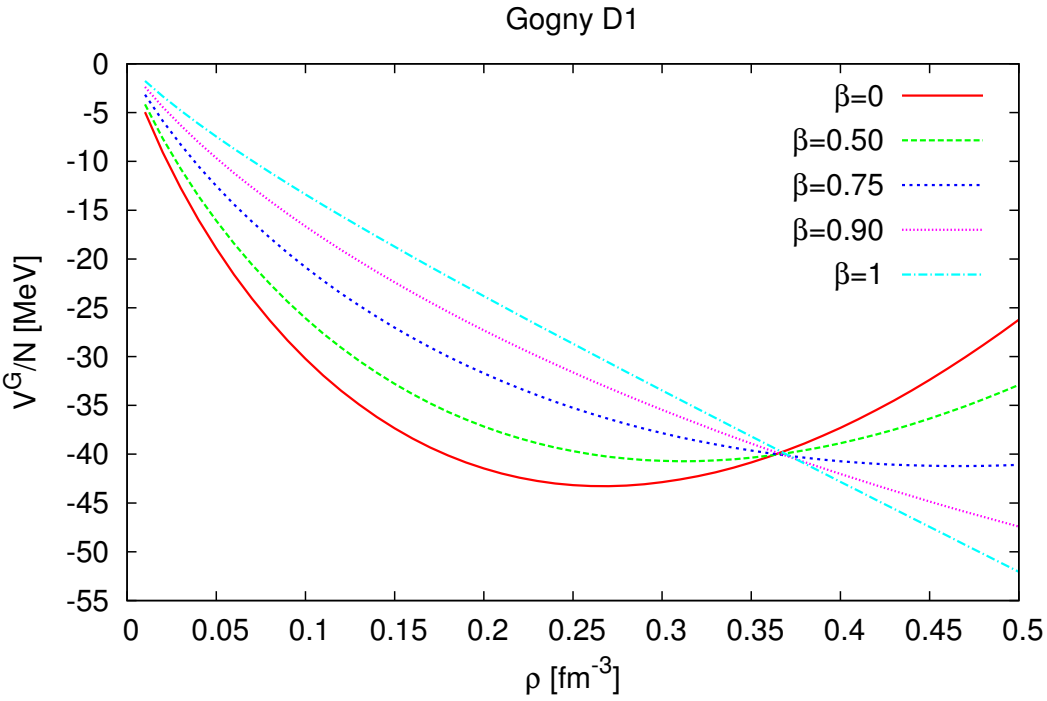


FIGURE 3.4: Gogny D1 potential energy per particle of non-polarized matter as a function of the total density for diffetent isospin asymmetry values.

asymmetry regardless of the spin polarization of the system. However, this statement is not true for the potential energy, for neither the Skyrme SLy4 nor the Gogny D1 interactions.

For the Skyrme SLy4, the potential energy of non-polarized and anti-polarized matter becomes more repulsive as the isospin asymmetry increases, whereas the potential energy of totally polarized matter becomes more attractive. Similarly, the Gogny D1 potential energy of anti-polarized matter becomes more repulsive as the isospin asymmetry increases and the opposite happens to the potential energy of totally polarized matter.

It is worth to point out the behaviour of the potential energy of non-polarized matter with the Gogny D1 interaction, showed in Fig. 3.4. There is a density value around $\rho \sim 0.365\,\mathrm{fm}^{-3}$ at which the potential energy per particle is almost independent of the isospin asymmetry. Therefore, the potential energy for non-polarized matter becomes more repulsive for density values $\rho \leq 0.365\,\mathrm{fm}^{-3}$ and becomes more attractive for density values $\rho \geq 0.365\,\mathrm{fm}^{-3}$ as the isospin asymmetry increases.

Let us now analyse the kinetic energy dependence on the spin polarization. We observe that the kinetic energy of non-polarized matter is smaller than that of totally and anti-polarized matter for any isospin asymmetry. This is a direct consequence of the Fermi character of the nucleon.

In a similar way, the potential energy of non-polarized matter is more

attractive than that of the fully polarized one, except for the Skyrme SLy4 potential energy of neutron matter, which presents a potential energy-crossing at $\rho \sim 0.46\,\mathrm{fm}^{-3}$, which lies outside of the figure.

For the Skyrme SLy4 interaction, the potential energy of anti-polarized matter is the most repulsive one at low densities and the most attractive one at large densities. In the case of the Gogny D1 interaction, the potential energy of anti-polarized matter is the most repulsive one up to a centain density. However, for large density values, the potential energy of fully polarized matter becomes the most repulsive one.

Notice that the potential energy of totally polarized neutron matter for the Skyrme SLy4 is zero, and it is almost zero for the Gogny D1 interaction (see Sec. 2.2). Thus, totally polarized neutron matter can be approximated to a free Fermi gas.

### 3.2.1 Potential Energy using the Slater Function

In many realistic situations, the interaction potential $\hat{v}(\mathbf{r}_1 - \mathbf{r}_2)$ only depends on the spatial coordinates. Then, it can be useful to perform the integration over momentum before the integration over the spatial coordinates to calculate the potential energy. This procedure is described below:

$$
\begin{aligned}
&\frac{1}{N}\,\langle \Psi_{FS}|\hat{V}|\Psi_{FS}\rangle = \\
&= \frac{1}{2N}\sum_{\sigma\sigma'\tau\tau'}\frac{\Omega^2}{(2\pi)^6}\int_{k_{F\sigma\tau}}\int_{k_{F\sigma'\tau'}} \mathrm{d}^3\mathbf{k}\,\mathrm{d}^3\mathbf{k}'\;\langle \mathbf{k}\sigma\tau,\mathbf{k}'\sigma'\tau'|\hat{v}(\mathbf{r}_1-\mathbf{r}_2)\hat{O}_\sigma\hat{O}_\tau|\mathbf{k}\sigma\tau,\mathbf{k}'\sigma'\tau'\rangle_A \\
&= \frac{1}{2N}\frac{1}{(2\pi)^6}\int \mathrm{d}^3\mathbf{r}_1\int \mathrm{d}^3\mathbf{r}_2\,\hat{v}(\mathbf{r}_1-\mathbf{r}_2)\sum_{\sigma\sigma'\tau\tau'}\int_{k_{F\sigma\tau}}\int_{k_{F\sigma'\tau'}}\mathrm{d}^3\mathbf{k}\,\mathrm{d}^3\mathbf{k}' \\
&\times\left[\langle\sigma\sigma'|\hat{O}_\sigma|\sigma\sigma'\rangle\;\langle\tau\tau'|\hat{O}_\tau|\tau\tau'\rangle - e^{-i\mathbf{k}\cdot(\mathbf{r}_1-\mathbf{r}_2)}e^{i\mathbf{k}'\cdot(\mathbf{r}_1-\mathbf{r}_2)}\,\langle\sigma\sigma'|\hat{O}_\sigma\hat{P}_\sigma|\sigma\sigma'\rangle\;\langle\tau\tau'|\hat{O}_\tau\hat{P}_\tau|\tau\tau'\rangle\right].
\end{aligned}
\tag{3.13}
$$

Using now

$$
\begin{aligned}
\int_{k_{F\sigma\tau}}\mathrm{d}^3\mathbf{k} &= (2\pi)^3\rho_{\sigma\tau}\,, \\
\int_{k_{F\sigma\tau}}\mathrm{d}^3\mathbf{k}\,e^{i\mathbf{k}'\cdot\mathbf{r}} &= (2\pi)^3\rho_{\sigma\tau}\ell(k_{F\sigma\tau}r)\,,
\end{aligned}
\tag{3.14}
$$

where $\nu_\sigma$ and $\nu_\tau$ are the spin and the isospin degeneracy, $\mathbf{r} = \mathbf{r}_1 - \mathbf{r}_2$ is the relative coordinate and $\ell(k_F r)$ is the so called Slater function,

$$
\ell(k_F r) = \frac{3j_1(k_F r)}{k_F r}\,, \qquad j_1(k_F r) = \frac{\sin(k_F r)}{(k_F r)^2} - \frac{\cos(k_F r)}{k_F r}\,. \tag{3.15}
$$

In the case of symmetric nuclear matter, one arrives to the following expression,

$$\frac{1}{N}\langle\Psi_{FS}|\hat{V}|\Psi_{FS}\rangle = \frac{\rho}{2}\frac{1}{\nu_\sigma^2\nu_\tau^2}\int \mathrm{d}^3\mathbf{r}\,\hat{v}(\mathbf{r}) \times \sum_{\sigma\sigma'\tau\tau'}\Big[\langle\sigma\sigma'|\hat{O}_\sigma|\sigma\sigma'\rangle\,\langle\tau\tau'|\hat{O}_\tau|\tau\tau'\rangle - \langle\sigma\sigma'|\hat{O}_\sigma\hat{P}_\sigma|\sigma\sigma'\rangle\,\langle\tau\tau'|\hat{O}_\tau\hat{P}_\tau|\tau\tau'\rangle\,\ell^2(k_F r)\Big], \tag{3.16}$$

which simplifies the calculation of the potential energy per particle to one integral over the relative coordinate and the corresponding traces and/or operators expected value.

We use this method as a check for our previous calculations on the Gogny interaction since it only depends on the relative coordinate, contrary to the Skyrme interaction which also has a momentum dependence. The resulting expressions from Eq. (3.16) for non-polarized, totally polarized and anti-polarized nuclear matter together with non-polarized and totally polarized neutron matter are reported in the appendix A.3.

In Fig. 3.5 we compare the calculations for the potential energy per particle integrating first over the momentum space (symbols) and the coordinates space (solid lines) for the potential energy per particle of non-polarized, totally polarized and anti-polarized nuclear matter and non-polarized and totally polarized neutron matter for the Gogny D1 interaction. This provides a non-trivial double-check of our numerical calculations.

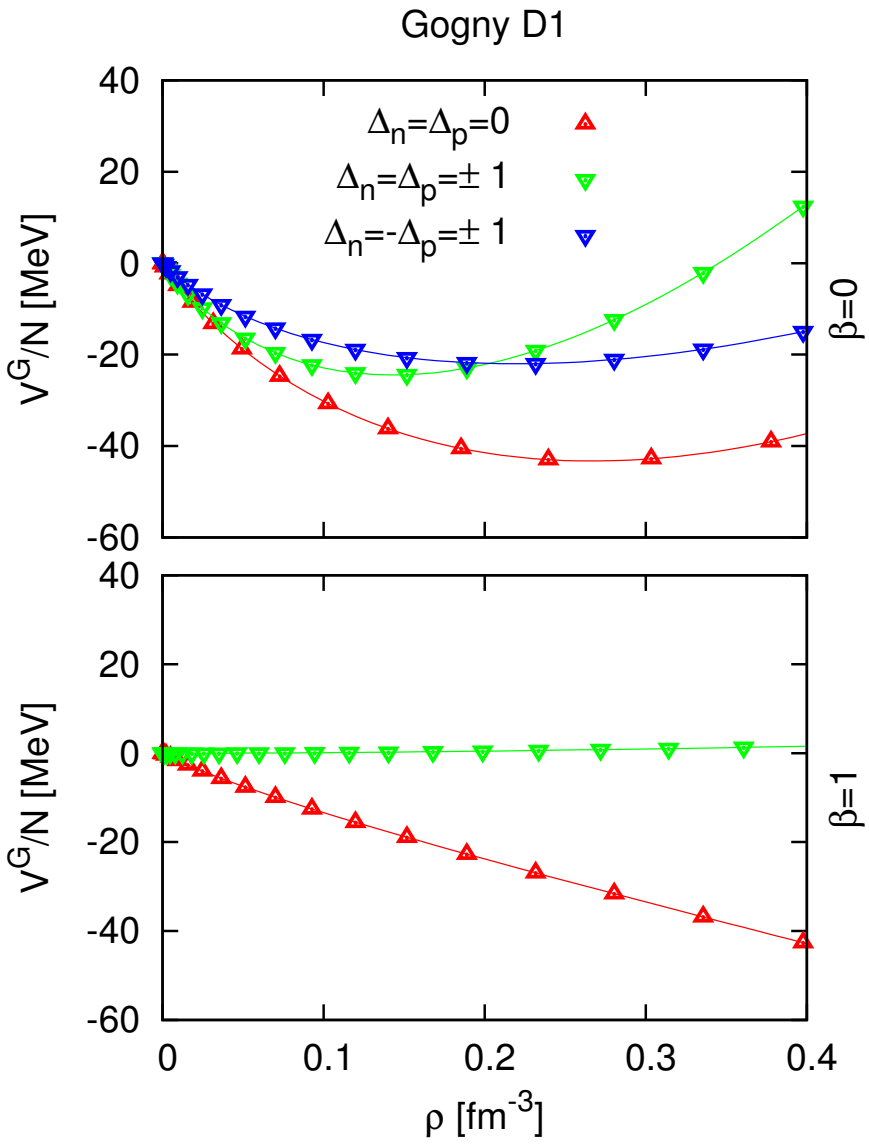


FIGURE 3.5: Potential energy per particle of symmetric nuclear matter (upper panel) and neutron matter (lower panel) for non-polarized ($\Delta_n = \Delta_p = 0$), totally polarized ($\Delta_n = \Delta_p \pm 1$) and anti-polarized ($\Delta_n = -\Delta_p \pm 1$) matter as functions of the total density for the Gogny D1 interaction. Symbols show the result for the calculation integrating first over the momentum space. Solid lines show the result for the calculation integrating first over the coordinates space.

## 3.3 Total Energy

Combining the expressions for the kinetic and potential energies, we can write down the expression for the total energy per particle for both the Skyrme and Gogny interactions.

For the Skyrme interaction, the total energy per particle is given by:

$$\begin{aligned}
e^{\mathrm{Sk}}(\rho_{n\uparrow},\rho_{n\downarrow},\rho_{p\uparrow},\rho_{p\downarrow}) = {} & \frac{\hbar^2}{2m_n}\frac{1}{\rho}[\xi_{n\uparrow}+\xi_{n\downarrow}] + \frac{\hbar^2}{2m_p}\frac{1}{\rho}[\xi_{p\uparrow}+\xi_{p\downarrow}] \\
& + \frac{1}{4\rho}[2t_2(1+x_2)][\xi_{n\uparrow}\rho_{n\uparrow}+\xi_{n\downarrow}\rho_{n\downarrow}+\xi_{p\uparrow}\rho_{p\uparrow}+\xi_{p\downarrow}\rho_{p\downarrow}] \\
& + \frac{1}{4\rho}[t_1(1-x_1)+t_2(1+x_2)][\xi_{n\uparrow}\rho_{n\downarrow}+\xi_{n\downarrow}\rho_{n\uparrow}+\xi_{p\uparrow}\rho_{p\downarrow}+\xi_{p\downarrow}\rho_{p\uparrow}] \\
& + \frac{1}{4\rho}[t_1(1+x_1)+t_2(1+x_2)][\xi_{n\uparrow}\rho_{p\uparrow}+\xi_{n\downarrow}\rho_{p\downarrow}+\xi_{p\uparrow}\rho_{n\uparrow}+\xi_{p\downarrow}\rho_{n\downarrow}] \\
& + \frac{1}{4\rho}[t_1+t_2][\xi_{n\uparrow}\rho_{p\downarrow}+\xi_{n\downarrow}\rho_{p\uparrow}+\xi_{p\uparrow}\rho_{n\downarrow}+\xi_{p\downarrow}\rho_{n\uparrow}] \\
& + \frac{1}{\rho}\left[t_0+\frac{1}{6}t_3\rho^{\gamma}\right]\rho_n\rho_p + \frac{1}{\rho}\left[t_0x_0+\frac{1}{6}t_3x_3\rho^{\gamma}\right][\rho_{n\uparrow}\rho_{p\uparrow}+\rho_{n\downarrow}\rho_{p\downarrow}] \\
& + \frac{1}{\rho}\left[t_0(1-x_0)+\frac{1}{6}t_3(1-x_3)\rho^{\gamma}\right][\rho_{n\uparrow}\rho_{n\downarrow}+\rho_{p\uparrow}\rho_{p\downarrow}]\,.
\end{aligned} \tag{3.17}$$

And the total energy per particle for the Gogny interaction is given by:

$$
\begin{aligned}
e^{\mathrm{G}}(\rho_{n\uparrow},\rho_{n\downarrow},\rho_{p\uparrow},\rho_{p\downarrow}) = \\
&= \frac{\hbar^2}{2m_n}\frac{1}{\rho}[\xi_{n\uparrow}+\xi_{n\downarrow}] + \frac{\hbar^2}{2m_p}\frac{1}{\rho}[\xi_{p\uparrow}+\xi_{p\downarrow}] \\
&+ \rho^{\gamma-1}t_0(1-x_0)(\rho_{n\uparrow}\rho_{n\downarrow}+\rho_{p\uparrow}\rho_{p\downarrow}) \\
&+ \rho^{\gamma-1}t_0\rho_n\rho_p + \rho^{\gamma-1}t_0x_0(\rho_{n\uparrow}\rho_{p\uparrow}+\rho_{n\downarrow}\rho_{p\downarrow}) \\
&+ \frac{\pi^{3/2}}{2\rho}\sum_i \mu_i^3\Big[W_i\rho^2 + B_i\big[(\rho_{n\uparrow}+\rho_{p\uparrow})^2+(\rho_{n\downarrow}+\rho_{p\downarrow})^2\big] \\
&\qquad - H_i(\rho_n^2+\rho_p^2) - M_i(\rho_{n\uparrow}^2+\rho_{n\downarrow}^2+\rho_{p\uparrow}^2+\rho_{p\downarrow}^2)\Big] \\
&- \frac{1}{4\rho\sqrt{\pi}}\sum_i\Big[(W_i+B_i-H_i-M_i)\Big(g_i(k_{Fn\uparrow},k_{Fn\uparrow})+g_i(k_{Fn\downarrow},k_{Fn\downarrow}) \\
&\qquad + g_i(k_{Fp\uparrow},k_{Fp\uparrow})+g_i(k_{Fp\downarrow},k_{Fp\downarrow})\Big) \\
&\qquad + (B_i-M_i)\Big(g_i(k_{Fn\uparrow},k_{Fn\downarrow})+g_i(k_{Fn\downarrow},k_{Fn\uparrow}) \\
&\qquad + g_i(k_{Fp\uparrow},k_{Fp\downarrow})+g_i(k_{Fp\downarrow},k_{Fp\uparrow})\Big) \\
&\qquad - (H_i+M_i)\Big(g_i(k_{Fn\uparrow},k_{Fp\uparrow})+g_i(k_{Fn\downarrow},k_{Fp\downarrow}) \\
&\qquad + g_i(k_{Fp\uparrow},k_{Fn\uparrow})+g_i(k_{Fp\downarrow},k_{Fn\downarrow})\Big) \\
&\qquad - M_i\Big(g_i(k_{Fn\uparrow},k_{Fp\downarrow})+g_i(k_{Fn\downarrow},k_{Fp\uparrow}) \\
&\qquad + g_i(k_{Fp\uparrow},k_{Fn\downarrow})+g_i(k_{Fp\downarrow},k_{Fn\uparrow})\Big)\Big]\,.
\end{aligned}
\tag{3.18}
$$

In Fig. 3.6 we present the total energy per particle as a function of the total density of symmetric nuclear matter (left column), asymmetric nuclear matter (central column) and neutron matter (right column) for different cases of spin polarization: non-polarized ($\Delta_n = \Delta_p = 0$), totally polarized ($\Delta_n = \Delta_p = \pm 1$) and anti-polarized ($\Delta_n = -\Delta_p = \pm 1$) nuclear matter, for both the Skyrme Sly4 and Gogny D1 interactions.

For the Gogny D1 interaction, non-polarized nuclear matter is always more attractive than totally and anti-polarized nuclear matter. However, for the Skyrme SLy4 interaction there is a crossing of the energy of non-polarized and anti-polarized nuclear matter at a density which increases with the isospin asymmetry. Thus, the anti-polarized nuclear matter can become the ground state at certain density regions [23, 24], when described with SLy4.

Concerning the preference of nuclear matter being totally polarized against anti-polarized we observe that both interactions predict the existence of a critical density ($\bar{\rho}$) such that for densities smaller than $\bar{\rho}$ the system prefers the totally polarized state and for larger densities than $\bar{\rho}$ the anti-polarized

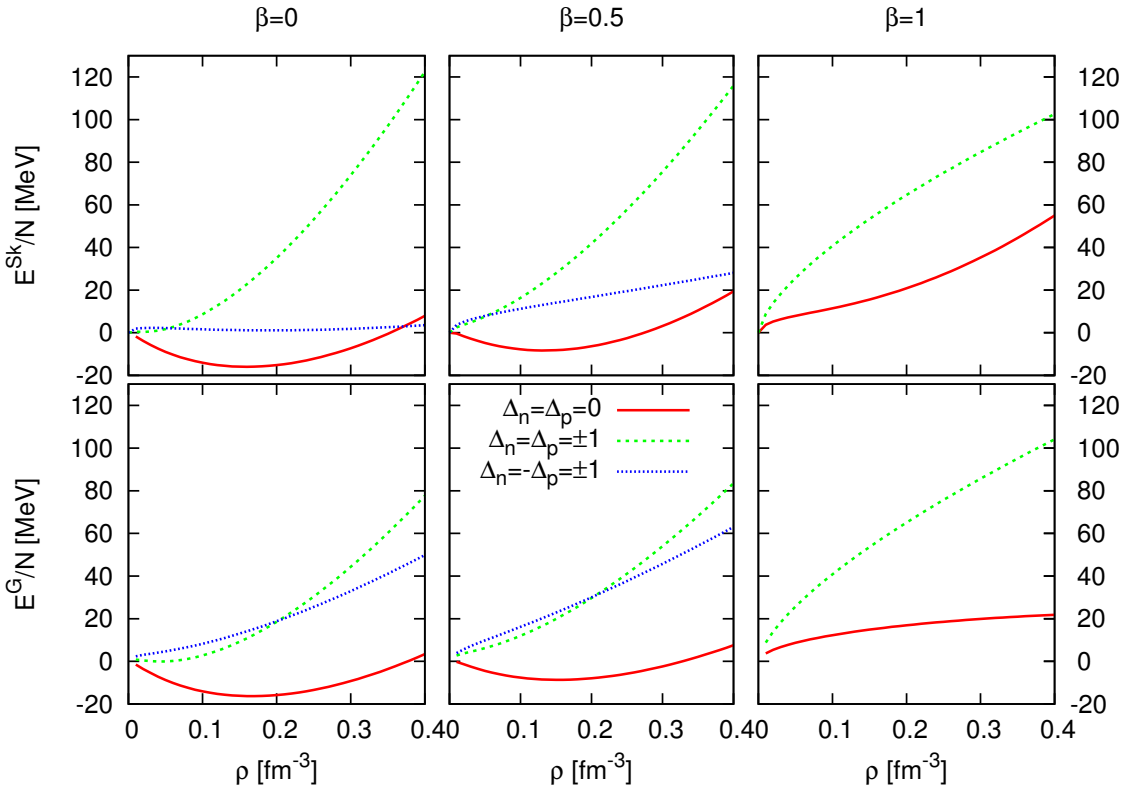


FIGURE 3.6: Total energy per particle for the Skyrme SLy4 interaction (upper row) and for the Gogny D1 interaction (lower row) as functions of the total density of symmetric nuclear matter (left column), asymmetric nuclear matter (central column) and neutron matter (right column) and non-polarized ($\Delta_n = \Delta_p = 0$), totally polarized ($\Delta_n = \Delta_p \pm 1$) and anti-polarized ($\Delta_n = -\Delta_p \pm 1$) nuclear matter.

state is preferred. The value of $\bar{\rho}$ increases with the asymmetry and it is always larger for the Gogny D1 interaction.

We oserve that the energy per particle of non-polarized symmetric matter for both the Skyrme SLy4 and Gogny D1 interactions is very similar and becomes more repulsive for large isospin asymmetries. However, they completly differ for non-polarized neutron matter.

Notice that for the case of totally polarized neutron matter both interactions predict similar results because, as we have already showed in Fig. 2.1 and Fig. 3.3, it can be approximated by a free Fermi gas.

### 3.3.1 Isospin symmetry energy

Since the energy per particle of non-polarized asymmetric nuclear matter is a function of the total density and the isospin asymmetry, it can generally be expressed as a Taylor expansion around $\beta = 0$. That is,

$$e(\rho, \beta) = e(\rho, 0) + e_{sym}(\rho)\beta^2 + e_4(\rho)\beta^4 + \mathcal{O}(\beta^6)\,. \tag{3.19}$$

Assuming charge symmetry of the nuclear forces, the interaction is symmetric under neutron and proton exchange and only even powers of $\beta$ appear in the expansion. $e_{sym}(\rho)$ is the so called symmetry energy and, if we only take the expansion up to second order, it can be approximated by,

$$e_{sym}(\rho) \sim e(\rho, 1) - e(\rho, 0)\,, \tag{3.20}$$

where $e(\rho, 1)$ and $e(\rho, 0)$ are the energy per particle of non-polarized neutron matter ($\beta = 1$) and for non-polarized symmetric nuclear matter ($\beta = 0$), respectively. Notice that a change of sign of $e_{sym}(\rho)$ would mean that there is a phase transition from nuclear to neutron matter.

In Fig. 3.7 we show the symmetry energy (solid line) for the Skyrme SLy4 interaction (left panel) and the Gogny D1 interaction (right panel) as functions of the total density. The total energy per particle (dotted lines) of non-polarized ($\Delta_n = \Delta_p = 0$) symmetric nuclear matter ($\beta = 0, \Delta_n = \Delta_p = 0$) and neutron matter ($\beta = 1$) are also plotted in the same figure.

The Skyrme SLy4 interaction shows no phase transition from nuclear matter to neutron matter at any value of the density. However, the Gogny D1 interaction does show a phase transition at $\rho_t \sim 0.52\,\text{fm}^{-3}$. This means that, for non-polarized matter, for $\rho > 0.52\,\text{fm}^{-3}$ the ground state ceases to be nuclear matter to become neutron matter.

The study of the symmetry energy of nuclear matter has also generated many theoretical works to analyse its density dependence around the saturation density and to understand the physical constraints imposed by experimental data [25, 26, 27, 28, 29].

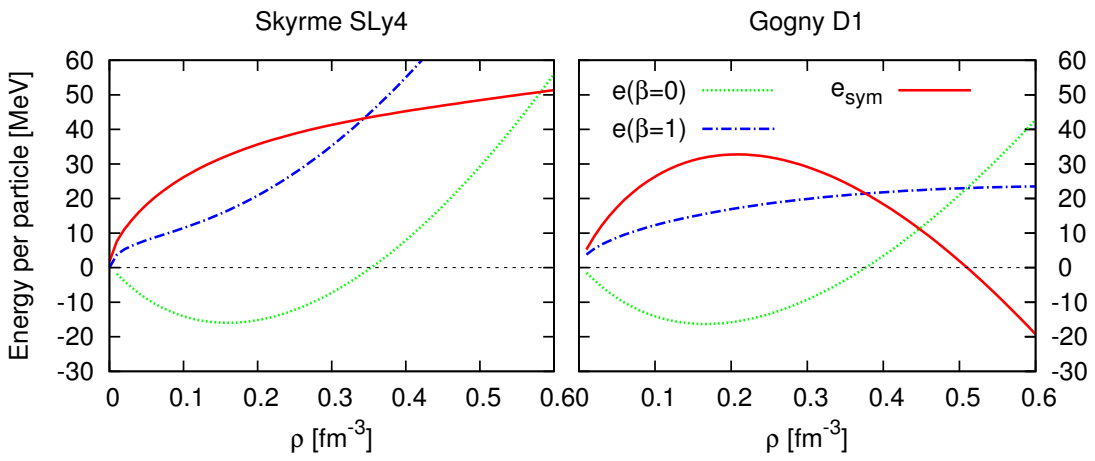


FIGURE 3.7: Isospin symmetry energy per particle (solid line) and total energy per particle (dotted lines) of non-polarized ($\Delta_n = \Delta_p = 0$) symmetric nuclear matter ($\beta = 0$) and neutron matter ($\beta = 1$) for the Skyrme SLy4 interaction (left panel) and the Gogny D1 interaction (right panel) as functions of the total density.

### 3.3.2 Spin symmetry energy

The energy per particle of spin-polarized neutron matter does not change when a global flip of the spins is performed. Therefore, it can be expanded on the spin polarization $\Delta_n$ as

$$e(\rho, \Delta_n) = e_0(\rho, 0) + S_{sym}(\rho)\Delta_n^2 + S_4(\rho)\Delta_n^4 + \mathcal{O}(\Delta_n^6)\,, \tag{3.21}$$

where $e_0(\rho, 0)$ is the energy per particle of non-polarized neutron matter ($\Delta_n = 0$) and $S_{sym}(\rho)$ is the so called spin symmetry energy,

$$S_{sym}(\rho) = \frac{1}{2}\left.\frac{\partial^2 e(\rho, \Delta_n)}{\partial \Delta_n^2}\right|_{\Delta_n = 0}\,. \tag{3.22}$$

If the dependence of the energy on the spin polarization is practically parabolic then the contributions from $\mathcal{O}(4)$ and higher orders can be neglected. Therefore, in this case, the spin symmetry energy can be estimated as the difference between the energy per particle of totally polarized ($\Delta_n = 1$) and non-polarized neutron matter ($\Delta_n = 0$),

$$S_{sym}(\rho) \sim e(\rho, 1) - e(\rho, 0)\,. \tag{3.23}$$

A change of sign of $S_{sym}(\rho)$ would indicate a ferromagnetic phase transition from non-polarized to totally polarized neutron matter.

In Fig. 3.8 we present the spin symmetry energy (solid line) for the Skyrme SLy4 interaction (left panel) and the Gogny D1 interaction (right panel) as a

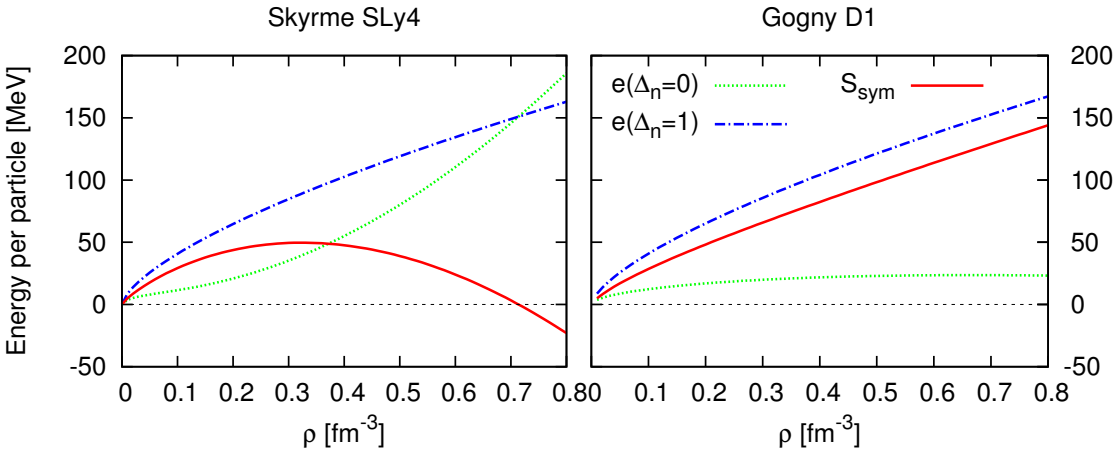


FIGURE 3.8: Spin symmetry energy per particle (solid line) and total energy per particle (dotted lines) of non-polarized ($\Delta_n = 0$) and totally polarized ($\Delta_n = 1$) neutron matter ($\beta = 1$) for the Skyrme SLy4 interaction (left panel) and the Gogny D1 interaction (right panel) as functions of the total density.

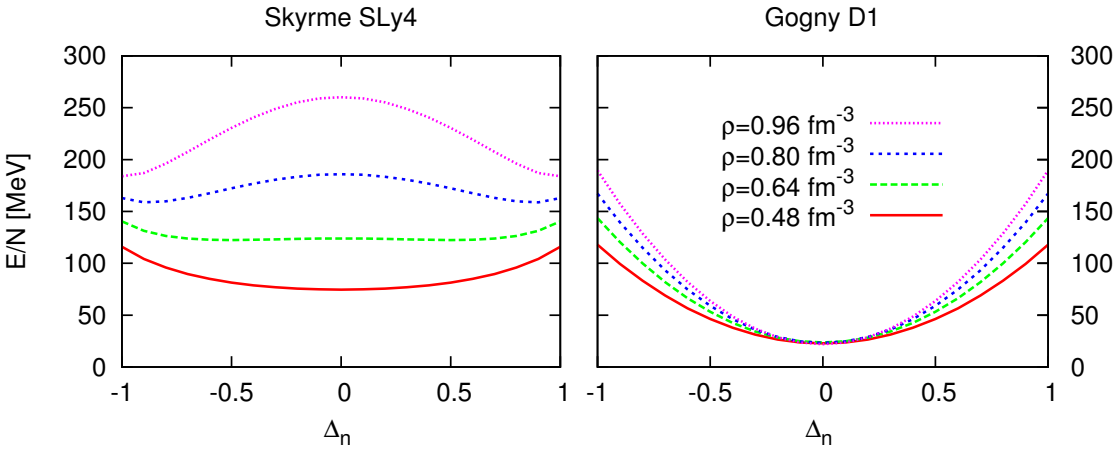


FIGURE 3.9: Total energy per particle of neutron matter ($\beta = 1$) at different densities for the Skyrme SLy4 interaction (left panel) and the Gogny D1 interaction (right panel) as a function of the neutron spin polarization.

functions of the total density. The total energy per particle (dotted lines) of non-polarized ($\Delta_n = 0$) and totally polarized ($\Delta_n = 1$) neutron matter ($\beta = 1$) are also plotted.

The Skyrme SLy4 interaction predicts a spin instability at $\rho_s \sim 0.72\,\text{fm}^{-3}$. Hence, non-polarized neutron matter is no longer the ground state of the system. The Gogny D1 interaction predicts no spin instability at any density. Therefore, the ground state is always non-polarized neutron matter.

In Fig. 3.9 we show the total energy per particle of neutron matter at different density values for the Skyrme SLy4 interaction (left panel) and the Gogny D1 interaction (right panel) as a function of the neutron spin polarization. We can see that for higher densities than a critical density $\rho_c = 0.6\,\text{fm}^{-3}$, provided by the magnetic susceptibility criteria (see Chapter 6), the Skyrme SLy4 interaction presents a spontaneous spin symmetry breaking where the non-polarized state is no longer stable, driving the system to a nonzero polarized state. Thus, the parabolic approximation is no longer valid [22]. A further increase of the density drives the system to a ferromagnetic state, i.e., totally polarized.

The Gogny D1 interaction keeps the parabolic behaviour as a function of the spin polarization in all the range of densities considered [30].

In Chapter 6 we discuss the spin instability of nuclear matter analyzing the magnetic susceptibility.

# Chapter 4

# Spin-Isospin Channel Contributions

The spin-isospin structure of the nucleon-nucleon interactions plays a very important role in describing the richness of the nucleon-nucleon scattering data and the structure of nuclei. To get further insight into the difference between the two forces we are considering, we discuss in this chapter the contribution to the potential energy of the different spin-isospin channels of the two-particle states.

The diagonal two-body matrix elements of the Skyrme interaction in terms of the spin-isospin channels are given by

$$\begin{aligned}\langle \mathbf{k}\mathbf{k}' S T M_S M_T | \hat{v}_{\text{Sk}}(\mathbf{r}) | \mathbf{k}\mathbf{k}' S T M_S M_T \rangle_A = \\ = \frac{1}{\Omega}\Bigg[ & t_0 + \frac{1}{6}t_3\rho^\gamma + \frac{1}{4}(\mathbf{k}-\mathbf{k}')^2(t_1+t_2) \\ & + \left\{ t_0 x_0 + \frac{1}{6}t_3 x_3 \rho^\gamma + \frac{1}{4}(\mathbf{k}-\mathbf{k}')^2(t_1 x_1 + t_2 x_2) \right\}(-1)^{S+1} \\ & - \left\{ t_0 + \frac{1}{6}t_3\rho^\gamma + \frac{1}{4}(\mathbf{k}-\mathbf{k}')^2(t_1 - t_2) \right\}(-1)^{S+T} \\ & - \left\{ t_0 x_0 + \frac{1}{6}t_3 x_3 \rho^\gamma + \frac{1}{4}(\mathbf{k}-\mathbf{k}')^2(t_1 x_1 - t_2 x_2) \right\}(-1)^{T+1} \Bigg] ,\end{aligned} \tag{4.1}$$

which lead to the following contributions of each spin-isospin channel to the potential energy per particle $\langle V_{ST} \rangle$) for polarized asymmetric nuclear matter:

$$\begin{aligned}\frac{\left\langle V_{11}^{\text{Sk}} \right\rangle}{N} = & \frac{1}{4}\Bigg\{ \frac{1}{4\rho}[2t_2(1+x_2)]\Big[ (\xi_{n\uparrow}+\xi_{n\downarrow}+\xi_{p\uparrow}+\xi_{p\downarrow})\rho + (\xi_{n\uparrow}+\xi_{n\downarrow})\rho_n + (\xi_{p\uparrow}+\xi_{p\downarrow})\rho_p \\ & + (\xi_{n\uparrow}+\xi_{p\uparrow})(\rho_{n\uparrow}+\rho_{p\uparrow}) + (\xi_{n\downarrow}+\xi_{p\downarrow})(\rho_{n\downarrow}+\rho_{p\downarrow}) \\ & + \xi_{n\uparrow}\rho_{n\uparrow} + \xi_{n\downarrow}\rho_{n\downarrow} + \xi_{p\uparrow}\rho_{p\uparrow} + \xi_{p\downarrow}\rho_{p\downarrow} \Big] \Bigg\} ;\end{aligned} \tag{4.2}$$

$$\frac{\langle V_{10}^{\rm Sk}\rangle}{N} = \frac{1}{2}\Bigg\{\frac{1}{\rho}\Bigg[t_0(1+x_0)+\frac{1}{6}t_3(1+x_3)\rho^\gamma\Bigg](\rho_n\rho_p+\rho_{n\uparrow}\rho_{p\uparrow}+\rho_{n\downarrow}\rho_{p\downarrow}) + \frac{1}{4\rho}[t_1(1+x_1)]\Big[\xi_{n\uparrow}\rho_{p\uparrow}+\xi_{n\downarrow}\rho_{p\downarrow}+\xi_{p\uparrow}\rho_{n\uparrow}+\xi_{p\downarrow}\rho_{n\downarrow} + (\xi_{n\uparrow}+\xi_{n\downarrow})\rho_p+(\xi_{p\uparrow}+\xi_{p\downarrow})\rho_n\Big]\Bigg\}; \tag{4.3}$$

$$\frac{\langle V_{01}^{\rm Sk}\rangle}{N} = \frac{1}{2}\Bigg\{\frac{1}{\rho}\Bigg[t_0(1-x_0)+\frac{1}{6}t_3(1-x_3)\rho^\gamma\Bigg]\Big[(\rho_{n\uparrow}+\rho_{p\uparrow})(\rho_{n\downarrow}+\rho_{p\downarrow})+\rho_{n\uparrow}\rho_{n\downarrow}+\rho_{p\uparrow}\rho_{p\downarrow}\Big] + \frac{1}{4\rho}[t_1(1+x_1)]\Big[\xi_{n\uparrow}\rho_{n\downarrow}+\xi_{n\downarrow}\rho_{n\uparrow}+\xi_{p\uparrow}\rho_{p\downarrow}+\xi_{p\downarrow}\rho_{p\uparrow} + (\xi_{n\uparrow}+\xi_{p\uparrow})(\rho_{n\downarrow}+\rho_{p\downarrow})+(\xi_{n\downarrow}+\xi_{p\downarrow})(\rho_{n\uparrow}+\rho_{p\uparrow})\Big]\Bigg\}; \tag{4.4}$$

$$\frac{\langle V_{00}^{\rm Sk}\rangle}{N} = \frac{1}{4}\Bigg\{\frac{1}{4\rho}[t_2(1-x_2)]\left(\xi_{n\uparrow}\rho_{p\downarrow}+\xi_{n\downarrow}\rho_{p\uparrow}+\xi_{p\uparrow}\rho_{n\downarrow}+\xi_{p\downarrow}\rho_{n\uparrow}\right)\Bigg\}. \tag{4.5}$$

Adding up together all the spin-isospin channel contributions in Eqs. (4.2)-(4.5) we recover the potential energy contribution in Eq. (3.10).

For the Gogny interaction, the spin-isospin structure of the diagonal two-body matrix elements of the Gogny reads

$$\begin{aligned}\langle \mathbf{k}\mathbf{k}' S T M_S M_T|\hat{v}_{\rm G}(\mathbf{r})|\mathbf{k}\mathbf{k}' S T M_S M_T\rangle_A = \\ = \frac{1}{\Omega}\Bigg\{&\rho^\gamma t_0\big[\big(1-(-1)^{S+T}\big)+x_0\big((-1)^{S+1}-(-1)^{T+1}\big)\big] \\ &+\pi^{3/2}\sum_i \mu_i^3\big[W_i+B_i(-1)^{S+1}-H_i(-1)^{T+1}-M_i(-1)^{S+T}\big] \\ &-\pi^{3/2}\sum_i \mu_i^3 e^{-\frac{\mu_i^2}{4}|\mathbf{q}|^2}\big[(-1)^{S+T}W_i+(-1)^{T+1}B_i-(-1)^{S+1}H_i-M_i\big]\Bigg\}.\end{aligned} \tag{4.6}$$

Then, the potential energy per particle in terms of the spin and isospin channels ($\langle V_{ST}\rangle$) is given by

$$\begin{aligned}
\frac{\langle V_{11}^{\rm G}\rangle}{N} &= \frac{\pi^{3/2}}{2\rho}\sum_i \mu_i^3[W_i + B_i - H_i - M_i] \\
&\times \left[\rho_{n\uparrow}^2 + \rho_{n\downarrow}^2 + \rho_{p\uparrow}^2 + \rho_{p\downarrow}^2 + \rho_{n\uparrow}\rho_{n\downarrow} + \rho_{p\uparrow}\rho_{p\downarrow} + \frac{1}{2}(\rho_{n\uparrow}\rho_{p\uparrow} + \rho_{n\downarrow}\rho_{p\downarrow} + \rho_n\rho_p)\right] \\
&- \frac{1}{4\rho\sqrt{\pi}}\sum_i [W_i + B_i - H_i - M_i] \\
&\times \Bigg[g_i(k_{Fn\uparrow}, k_{Fn\uparrow}) + g_i(k_{Fn\downarrow}, k_{Fn\downarrow}) + g_i(k_{Fp\uparrow}, k_{Fp\uparrow}) + g_i(k_{Fp\downarrow}, k_{Fp\downarrow}) \\
&+ \frac{1}{2}\Big(g_i(k_{Fn\uparrow}, k_{Fp\uparrow}) + g_i(k_{Fn\downarrow}, k_{Fp\downarrow}) + g_i(k_{Fp\uparrow}, k_{Fn\uparrow}) + g_i(k_{Fp\downarrow}, k_{Fn\downarrow}) \\
&+ g_i(k_{Fn\uparrow}, k_{Fn\downarrow}) + g_i(k_{Fn\downarrow}, k_{Fn\uparrow}) + g_i(k_{Fp\uparrow}, k_{Fp\downarrow}) + g_i(k_{Fp\downarrow}, k_{Fp\uparrow})\Big) \\
&+ \frac{1}{4}\Big(g_i(k_{Fn\uparrow}, k_{Fp\downarrow}) + g_i(k_{Fn\downarrow}, k_{Fp\uparrow}) + g_i(k_{Fp\uparrow}, k_{Fn\downarrow}) + g_i(k_{Fp\downarrow}, k_{Fn\uparrow})\Big)\Bigg];
\end{aligned} \tag{4.7}$$

$$\begin{aligned}
\frac{\langle V_{10}^{\rm G}\rangle}{N} &= \frac{1}{2}\rho^{\gamma-1}t_0[1 + x_0][\rho_{n\uparrow}\rho_{p\uparrow} + \rho_{n\downarrow}\rho_{p\downarrow} + \rho_n\rho_p] \\
&+ \frac{1}{2}\frac{\pi^{3/2}}{2\rho}\sum_i \mu_i^3[W_i + B_i + H_i + M_i](\rho_{n\uparrow}\rho_{p\uparrow} + \rho_{n\downarrow}\rho_{p\downarrow} + \rho_n\rho_p) \\
&- \frac{1}{4\rho\sqrt{\pi}}\sum_i [-W_i - B_i - H_i - M_i] \\
&\times \Bigg[\frac{1}{2}\Big(g_i(k_{Fn\uparrow}, k_{Fp\uparrow}) + g_i(k_{Fn\downarrow}, k_{Fp\downarrow}) + g_i(k_{Fp\uparrow}, k_{Fn\uparrow}) + g_i(k_{Fp\downarrow}, k_{Fn\downarrow})\Big) \\
&+ \frac{1}{4}\Big(g_i(k_{Fn\uparrow}, k_{Fp\downarrow}) + g_i(k_{Fn\downarrow}, k_{Fp\uparrow}) + g_i(k_{Fp\uparrow}, k_{Fn\downarrow}) + g_i(k_{Fp\downarrow}, k_{Fn\uparrow})\Big)\Bigg];
\end{aligned} \tag{4.8}$$

$$\begin{aligned}
\frac{\langle V_{01}^{\rm G}\rangle}{N} &= \frac{1}{2}\rho^{\gamma-1}t_0[1 - x_0]\Big[\rho_{n\uparrow}\rho_{n\downarrow} + \rho_{p\uparrow}\rho_{p\downarrow} + (\rho_{n\uparrow} + \rho_{p\uparrow})(\rho_{n\downarrow} + \rho_{p\downarrow})\Big] \\
&+ \frac{1}{2}\frac{\pi^{3/2}}{2\rho}\sum_i \mu_i^3[W_i - B_i - H_i + M_i]\Big[\rho_{n\uparrow}\rho_{n\downarrow} + \rho_{p\uparrow}\rho_{p\downarrow} + (\rho_{n\uparrow} + \rho_{p\uparrow})(\rho_{n\downarrow} + \rho_{p\downarrow})\Big] \\
&- \frac{1}{4\rho\sqrt{\pi}}\sum_i [-W_i + B_i + H_i - M_i] \\
&\times \Bigg[\frac{1}{2}\Big(g_i(k_{Fn\uparrow}, k_{Fn\downarrow}) + g_i(k_{Fn\downarrow}, k_{Fn\uparrow}) + g_i(k_{Fp\uparrow}, k_{Fp\downarrow}) + g_i(k_{Fp\downarrow}, k_{Fp\uparrow})\Big) \\
&+ \frac{1}{4}\Big(g_i(k_{Fn\uparrow}, k_{Fp\downarrow}) + g_i(k_{Fn\downarrow}, k_{Fp\uparrow}) + g_i(k_{Fp\uparrow}, k_{Fn\downarrow}) + g_i(k_{Fp\downarrow}, k_{Fn\uparrow})\Big)\Bigg];
\end{aligned} \tag{4.9}$$

$$\frac{\langle V_{00}^{\rm G}\rangle}{N} = \frac{1}{2}\frac{\pi^{3/2}}{2\rho}\sum_i \mu_i^3[W_i - B_i + H_i - M_i][\rho_{n\uparrow}\rho_{p\downarrow} + \rho_{n\downarrow}\rho_{p\uparrow}] - \frac{1}{4}\frac{1}{4\rho\sqrt{\pi}}\sum_i [W_i - B_i + H_i - M_i] \times \Big[g_i(k_{Fn\uparrow}, k_{Fp\downarrow}) + g_i(k_{Fn\downarrow}, k_{Fp\uparrow}) + g_i(k_{Fp\uparrow}, k_{Fn\downarrow}) + g_i(k_{Fp\downarrow}, k_{Fn\uparrow})\Big] . \tag{4.10}$$

Again, adding up together all spin-isospin channel contributions in Eqs. (4.7)-(4.10) we recover Eq. (3.11).

One can still perform an additional decomposition by analysing the contribution to the potential energy of the different third components of the spin-isospin two-body states. The expressions can be found in appendix A.4.

In Fig.4.1 and Fig. 4.2 are shown the contributions of each channel (dotted lines) to the potential energy per particle (solid line) for different values of the isospin asymmetry ($\beta$) and the spin polarizations ($\Delta_n, \Delta_p$) for both the Skyrme and Gogny interactions, respectively.

Looking at Eqs. (4.2)-(4.5), Eqs. (4.7)-(4.10) and Fig. 4.1 and Fig. 4.2, one can see that the contribution of the channel $\langle V_{11}\rangle$ is zero by construction for the Skyrme SLy4 as imposed in the parametrization of the force. For the Gogny D1 interaction $\langle V_{11}\rangle$ is not strictly zero, but really small compared to the other contributing channels.

The contribution of $T = 0$ channels, $\langle V_{10}\rangle$ and $\langle V_{00}\rangle$, decrease when the asymmetry increases and become zero for neutron matter. Similarly, the $S = 0$ channels, $\langle V_{01}\rangle$ and $\langle V_{00}\rangle$, do not contribute for totally polarized matter. $\langle V_{00}\rangle$ only contributes for nuclear matter when nucleons have different spin polarizations. It might seem zero for the Gogny D1 interaction, but it does contribute within the proper conditions, just as $\langle V_{11}\rangle$.

## 4.1 Partial Wave Decomposition

A deeper insight in the understanding on the interaction can be obtained by performing a partial wave decomposition of the interaction energy. This can be useful to compare different interactions and enlighten the differences with realistic interactions.

It is convenient to express the two-body states in terms of the center of mass and the relative motion.

$$\begin{aligned}|\mathbf{K}_{CM}\mathbf{k}_r STM_S M_T\rangle &= \frac{1}{\Omega}e^{i\mathbf{K}_{CM}\mathbf{R}}e^{i\mathbf{k}_r\mathbf{r}}\chi^S_{M_S}\chi^T_{M_T} \\ &= \frac{1}{\Omega}e^{i\mathbf{K}_{CM}\mathbf{R}}4\pi\sum_{\ell m} i^\ell j_\ell(kr)Y^*_{\ell m}(\hat{k})Y_{\ell m}(\hat{r})\chi^S_{M_S}\chi^T_{M_T}\,,\end{aligned} \tag{4.11}$$

where $\mathbf{r} = \mathbf{r}_1 - \mathbf{r}_2$ is the relative coordinate between, $\mathbf{R} = (\mathbf{r}_1 + \mathbf{r}_2)/2$ is the center of mass coordinate, $\mathbf{k}_r = \mathbf{k} - \mathbf{k}'$ is the relative momentum, $\mathbf{K}_{CM} = (\mathbf{k} + \mathbf{k}')/2$ is the center of mass momentum. The plane wave associated to the

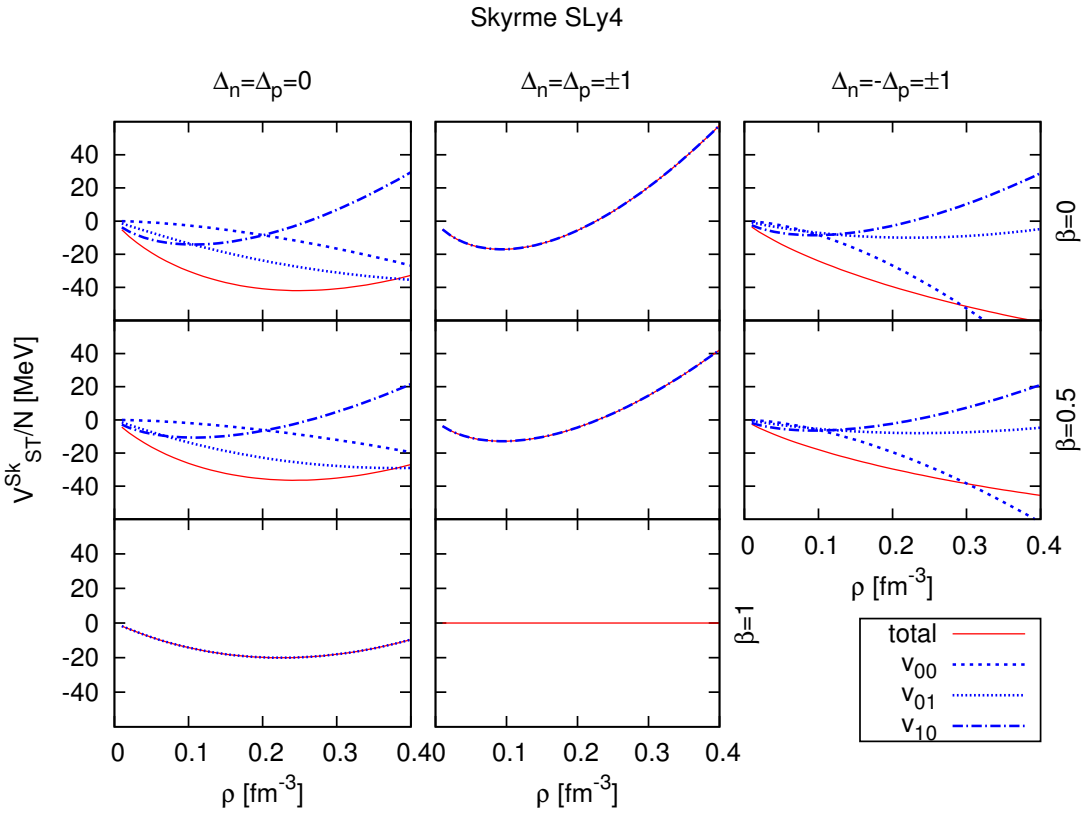


FIGURE 4.1: Skyrme SLy4 interaction potential energy per particle spin-isospin channel contributions for symmetric nuclear matter (upper row), asymmetric nuclear matter with $\beta = 0.5$ (middle row) and neutron matter (lower row) and non-polarized (left column), totally polarized (center column) and anti-polarized (right column) matter as functions of total density. Solid line shows the total potential energy per particle. Dotted lines show the spin-isospin channel contributions. Non-contributing channels are not plotted. $\langle V_{11} \rangle$ never appears because it is set to zero by SLy4.

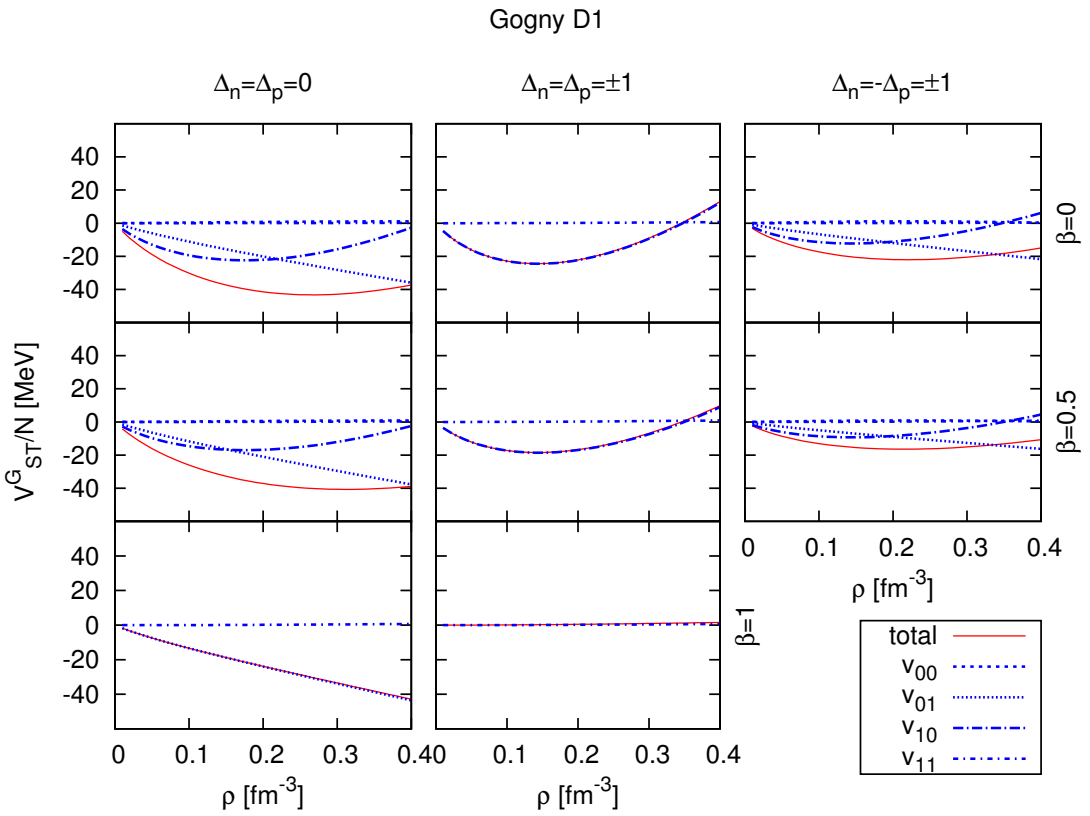


FIGURE 4.2: Gogny D1 interaction potential energy per particle spin-isospin channel contributions for symmetric nuclear matter (upper row), asymmetric nuclear matter with $\beta = 0.5$ (middle row) and neutron matter (lower row) and non-polarized (left column), totally polarized (center column) and anti-polarized (right column) matter as functions of total density. Solid line shows the total potential energy per particle. Dotted lines show the spin-isospin channel contributions. Non-contributing channels are not plotted.

relative momentum is expressed in terms of the different potential waves, characterized by their angular momentum, $\ell$ with the help of the Bessel functions $j_\ell(kr)$ and the spherical harmonics $Y^*_{\ell m}$.

The antisymmetrization of the two-body state acts only on the relative motion, and the spin and isospin wave functions, see Eq. (2.13), results in

$$|\mathbf{K}_{CM}\mathbf{k}_r STM_S M_T\rangle_A = \frac{1}{\Omega} e^{i\mathbf{KR}} 4\pi \sum_{\ell m} i^\ell j_\ell(kr)\big(1-(-1)^{\ell+S+T}\big) Y^*_{\ell m}(\hat{k}) Y_{\ell m}(\hat{r}) \chi^S_{M_S}\chi^T_{M_T}\,. \tag{4.12}$$

Thus, not all partial wave functions are allowed, and only those with $\ell+S+T$ odd are permitted.

First, we calculate the contribution of the coefficient partial waves to the single-particle potential, which is given by:

$$\begin{aligned}
U(k) &= \frac{1}{\nu_\sigma\nu_\tau}\sum_{k'\le k'_F}\sum_{SM_S}\sum_{TM_T} {}_A\langle \mathbf{k}\mathbf{k}' STM_S M_T|v(\mathbf{r})|\mathbf{k}\mathbf{k}' STM_S M_T\rangle_A \\
&= \frac{1}{\nu_\sigma\nu_\tau}\frac{\Omega}{(2\pi)^3}\int_{k'\le k'_F} \mathrm{d}^3k' \left(\frac{1}{\Omega}\int e^{-i\mathbf{KR}} e^{i\mathbf{KR}} d^3R\right)\times \\
&\times \sum_{SM_S TM_T}\sum_{\ell m\ell' m'} (4\pi)^2\big(1-(-1)^{\ell+S+T}\big) Y_{\ell m}(\hat{k}) Y_{\ell' m}(\hat{k}) \chi^{S*}_{M_S}\chi^S_{M_S}\chi^{T*}_{M_T}\chi^T_{M_T}\times \\
&\times i^{\ell'-\ell}\frac{1}{\Omega}\int \mathrm{d}r\, r^2 j_\ell(kr) v(r) j'_\ell(kr)\int Y_{\ell m}(\hat{r}) Y_{\ell' m}(\hat{r}) d\Omega_r \\
&= \frac{1}{\nu_\sigma\nu_\tau}\frac{1}{(2\pi)^3}\sum_{\ell ST} 4\pi(2\ell+1)(2S+1)(2T+1)\big(1-(-1)^{\ell+S+T}\big)\times \\
&\qquad \times \int_{k'\le k'_F}\mathrm{d}^3k' \int \mathrm{d}r\, r^2 j_\ell(kr) v(r) j'_\ell(kr)\,.
\end{aligned} \tag{4.13}$$

It is convenient to define

$$V^\ell_{k_r} = \frac{2}{\pi}\int \mathrm{d}r\, r^2 j_\ell(kr) v(r) j_\ell(kr)\,, \tag{4.14}$$

which corresponds to the diagonal matrix elements of the interaction in momentum space for the different partial waves. Using $V^\ell_{k_r}$, the single-particle potential reads

$$U(k) = \frac{1}{\nu_\sigma\nu_\tau}\frac{1}{2\pi^2}\frac{\pi}{2}\sum_{\ell ST}(2\ell+1)(2S+1)(2T+1)\big(1-(-1)^{\ell+S+T}\big)\int_{k'\le k'_F}\mathrm{d}^3k'\, V^\ell_{k_r}\,. \tag{4.15}$$

Notice that the integral is extended to all momenta $\mathbf{k}'$ inside the Fermi sphere and that in the numerical procedure to compute $U(k)$ we need to determine the relative momentum $\mathbf{k}_r$ associated to each external momentum $k$ (located at the Z-axis) and each internal momentum $\mathbf{k}'$.

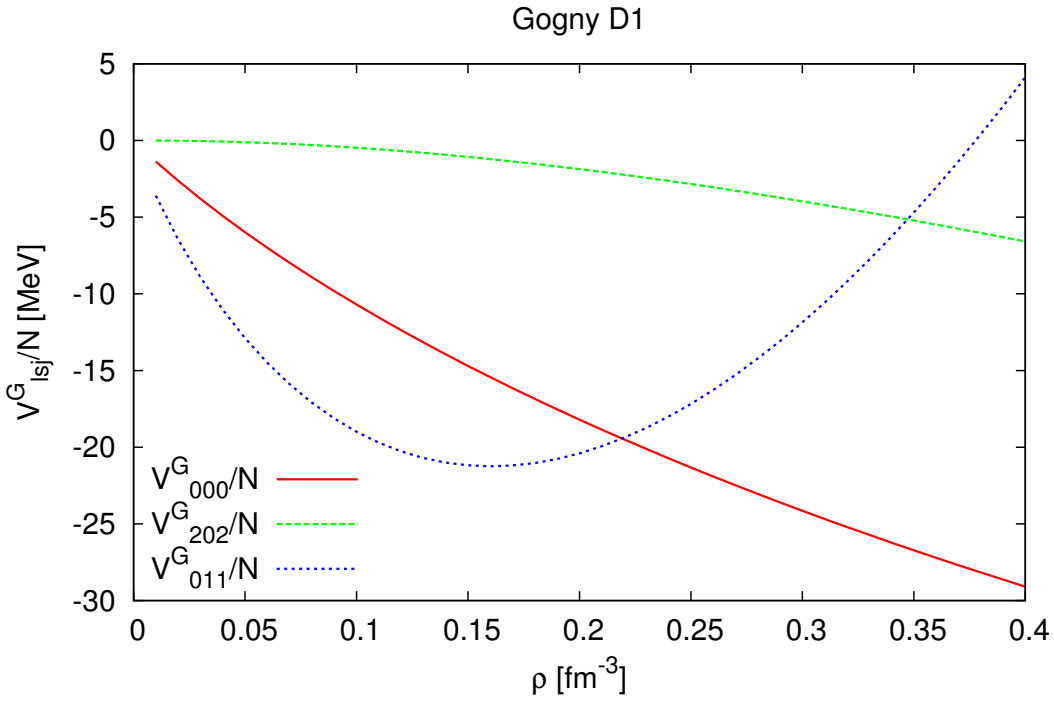


FIGURE 4.3: Potential energy per particle contributions of the partial waves that contribute the most ($\ell sj = 000, 202, 011$) as a function of density for the Gogny D1 interaction.

Once we have the single-particle potential, which for non-polarized symmetric nuclear matter is the same regardless of the spin and isospin component of the nucleon, we can easily compute the total potential energy by integrating $U(k)$ inside the Fermi sphere and adding a $\frac{1}{2}$ factor to avoid the double-counting.

In Fig. 4.3 we show the partial waves that contribute the most to the potential energy per particle as functions of density for the Gogny D1 interaction. These partial waves correspond to the quantum numbers $\ell Sj = 000, 202, 011$ which define the partial waves $(^{2S+1}\ell_j)$ $^1S_0$,$^1D_2$,$^3S_1$, respectively, being $j$ the total angular momentum.

The contribution of all depicted partial wave is attractive in a wide range of densities. The partial wave $\ell = 0$ collects the main contributions. As $\ell$ increases, this contributions decrease rather rapidly. The addition of all partial waves restore the results obtained previously. Notice also that the contribution of $\ell = 1$ is much smaller than the $\ell = 2$. Here is also useful to remind that for the Skyrme interaction, including the gradient terms we only have $S$ and $P$ waves.

It is the presence of the finite range in the Gogny force that allows to have contributions of higher partial waves.

# Chapter 5

# Interaction Potential Parametrization

In order to qualitatively understand the effect of neutron and proton spin polarizations and isospin asymmetry on the potential energy contribution, one can analyse the partial contributions of the single-particle potential $U_{\sigma\tau\sigma'\tau'}(k)$ to single out explicitly the dependence on the phase space [31]:

$$U_{\sigma\tau\sigma'\tau'}(k) = g_{\sigma\tau\sigma'\tau'}\rho_{\sigma'\tau'}\,, \tag{5.1}$$

where $g_{\sigma\tau\sigma'\tau'}$ is the average value of the matrix element $\langle \mathbf{k}\sigma\tau, \mathbf{k}'\sigma'\tau'|\hat{v}|\mathbf{k}\sigma\tau, \mathbf{k}'\sigma'\tau'\rangle_A$ in the Fermi sphere with radius $k' \leq k'_{F\sigma'\tau'}$. The density factor $\rho_{\sigma'\tau'}$ arises from the integral over the corresponding Fermi sea.

For small values of the asymmetry ($\beta \ll 1$) and the neutron and proton spin polarizations ($|\Delta_n|, |\Delta_p| \ll 1$), one can neglect the dependence on $\beta, \Delta_n$ and $\Delta_p$ assuming $g_{\sigma\tau\sigma'\tau'} \sim g_{\sigma\tau\sigma'\tau'}(k,\rho)$ and

$$g_{\sigma\tau\sigma\tau} = g_1 \qquad g_{\sigma\tau\sigma'\tau} = g_2 \qquad g_{\sigma\tau\sigma\tau'} = g_3 \qquad g_{\sigma\tau\sigma'\tau'} = g_4 \qquad . \tag{5.2}$$

with $\sigma \neq \sigma'\,, \tau \neq \tau'$.

With these assumptions, we can express Eq. (3.8) in terms of Eq. (5.1), as

$$\frac{\langle V\rangle}{N} = \frac{1}{2N}\sum_{\sigma\sigma'}\sum_{\tau\tau'}\sum_{k\leq k_{F\sigma\tau}} g_{\sigma\tau\sigma'\tau'}(k,\rho)\rho_{\sigma'\tau'}\,. \tag{5.3}$$

After performing the averages of $g_i(k,\rho)$ over the Fermi sphere of radius $k_{\sigma\tau}$ and after some algebra, one arrives to

$$\begin{aligned}\frac{\langle V\rangle}{N} \approx{}& \frac{\rho^2}{4}(\bar{g}_1+\bar{g}_2+\bar{g}_3+\bar{g}_4) + \frac{\rho^2}{4}(\bar{g}_1+\bar{g}_2-\bar{g}_3-\bar{g}_4)\beta^2 \\ &+ \frac{\rho^2}{8}(\bar{g}_1-\bar{g}_2)(1+\beta)^2\Delta_n^2 + \frac{\rho^2}{8}(\bar{g}_1-\bar{g}_2)(1-\beta)^2\Delta_p^2 \\ &+ \frac{\rho^2}{4}(\bar{g}_3-\bar{g}_4)(1-\beta^2)\Delta_n\Delta_p\,.\end{aligned} \tag{5.4}$$

Thus, we can write the total energy per particle as a function of the parameters $\beta, \Delta_n$ and $\Delta_p$ using Eq. (A.10) and Eq .(5.4):

$$\begin{aligned} e(\rho,\beta,\Delta_n,\Delta_p) = \frac{\langle T\rangle}{N}(\rho,\beta,\Delta_n,\Delta_p) + V_0(\rho) + V_1(\rho)\beta^2 \\ + V_2(\rho)(1+\beta)^2\Delta_n^2 + V_2(\rho)(1-\beta)^2\Delta_p^2 \\ + V_3(\rho)(1-\beta^2)\Delta_n\Delta_p\,. \end{aligned} \tag{5.5}$$

The coefficients $V_0(\rho), V_1(\rho), V_2(\rho)$ and $V_3(\rho)$ (see Fig. 5.1) have been determined as follows:

$$\begin{aligned} V_0 &= \frac{\langle V\rangle}{N}(\beta=0,\Delta_n=0,\Delta_p=0)\,, \\ V_1 &= \frac{\langle V\rangle}{N}(\beta=1,\Delta_n=0,\Delta_p=0) - V_0\,, \\ V_2 &= \frac{\langle V\rangle}{N}(\beta=0,\Delta_n=1,\Delta_p=0) - V_0\,, \\ V_3 &= \frac{\langle V\rangle}{N}(\beta=0,\Delta_n=1,\Delta_p=1) - V_0 - 2V_2\,. \end{aligned} \tag{5.6}$$

This parametrization is consistent with the spin and isospin structure of the nucleon-nucleon interaction in the sense that, for a given configuration of $\beta, \Delta_n$ and $\Delta_p$, a global spin-flip does not change the energy whereas a flip only over all neutrons or protons spins does.

The dependence on the density of $V_i(\rho)$ coefficients is shown in Fig. 5.1 for both interactions. The behaviour of $V_0$ and $V_2$ is rather similar for both interactions. However, $V_1$ and $V_3$ show a very different behaviour.

In Fig. 5.2 we test the quality of the previously defined fit by comparing the total energy per particle, as a function of proton spin polarization ($\Delta_p$), provided by Eq. (5.5) and the exact total energy expressions, see Eq. (3.17) and Eq. (3.18). The comparison is performed per particle for the Skyrme SLy4 interaction (upper row) and Gogny D1 interaction (lower row) for different values of the neutron spin polarization ($\Delta_n = 0, 0.5, 0.75, 1$) and different isospin asymmetries ($\beta = 0.25, 0.5$) at saturation density $\rho_0 = 0.16\,\mathrm{fm}^{-3}$. In general, the parametrization reproduces successfully the exact results. However, it worsens when the asymmetry and/or the polarizations become large.

The goodness of the parametrization as a function of the density for different asymmetries and polarization is shown for both interactions in Fig. 5.3. We observe an overall agreement that worsens beyond the assumptions defined to perform the parametrization.

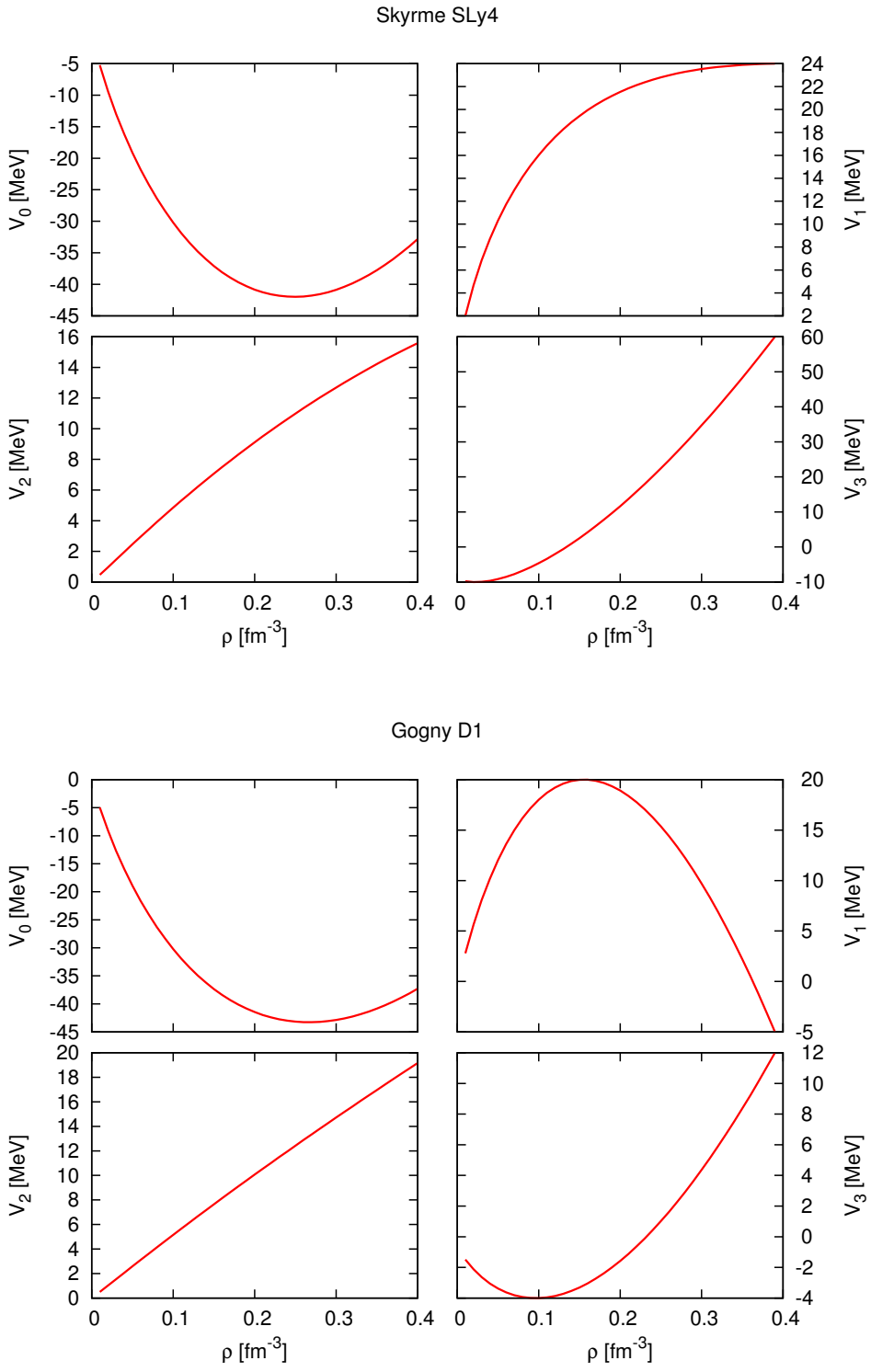


FIGURE 5.1: Skyrme SLy4 interaction (top panels) and Gogny D1 interaction (lower panels) potential parameters from Eq. (5.6) as functions of total density.

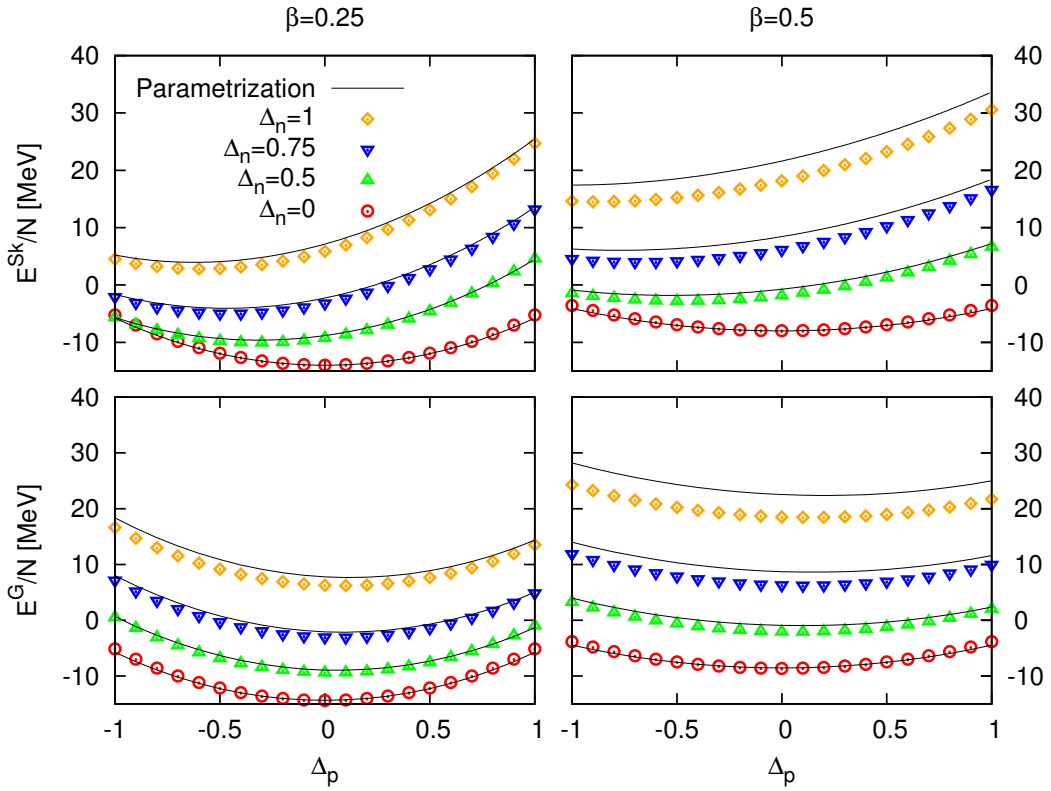


FIGURE 5.2: Total energy per particle as function of proton spin polarization ($\Delta_p$) for Skyrme SLy4 interaction (upper row) and Gogny D1 interaction (lower row) for different values of the neutron spin polarization ($\Delta_n = 0, 0.5, 0.75, 1$) and different isospin asymmetries ($\beta = 0.25, 0.5$) at saturation density $\rho_0 = 0.16\,\mathrm{fm}^{-3}$. Symbols show the results for the exact calculations. Solid line shows the results for the parametrization in Eq. (5.5).

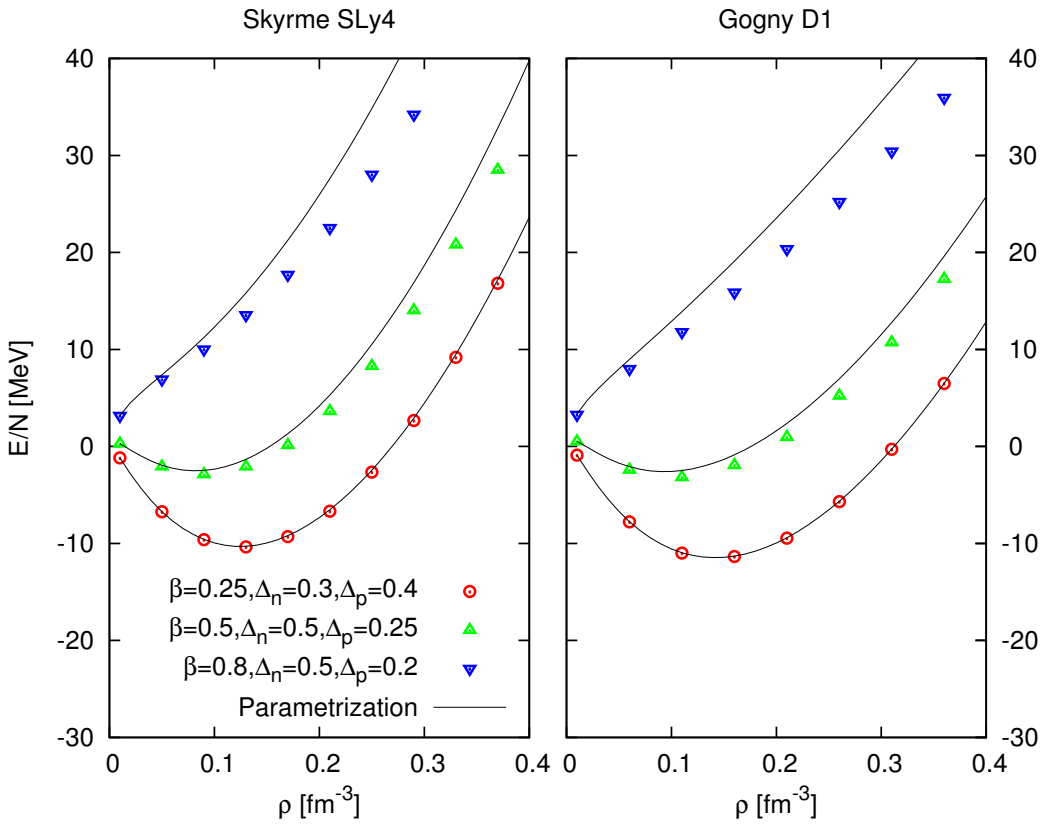


FIGURE 5.3: Total energy per particle as function of density for Skyrme SLy4 interaction (top) and Gogny D1 interaction (bottom) for different values of the neutron and proton spin polarizations ($\Delta_n, \Delta_p$) and different isospin asymmetries ($\beta$) at saturation density $\rho_0 = 0.16\,\mathrm{fm}^{-3}$. Symbols show the results for the exact calculations. Solid lines show the results for the parametrization in Eq. (5.5).

# Chapter 6

# Magnetic Susceptibility

In the astrophysical context, pulsars are known to be rapidly rotating neutron stars with an intense magnetic field [32, 33, 34, 35]. Therefore, the possibility of phase transition to a ferromagnetic state in neutron matter has been a field of study that still presents some contradictory results. This transition could have important consequences for the evolution of protoneutron stars, in particular for the spin correlations in the medium that strongly affect the neutrino cross-sections and mean free paths inside the star [36].

Some studies done with microscopic calculations show that there is no possible ferromagnetic phase transition [31, 37, 38, 39, 40, 41, 42, 43, 44, 45], and so do others using effectives forces [30, 46]. On the other hand, calculations using different effective forces do find a ferromagnetic phase transition [22, 47]. Some of the results are, however, merely academic since they cannot be reached by protoneutron stars.

The magnetic susceptibility $\chi(\rho)$ characterizes the response of the system to an external magnetic field and gives a measure of the energy required to produce a net spin alignment in the direction of the field. For nuclear matter, it is defined as a $2 \times 2$ matrix

$$\frac{1}{\chi} = \begin{pmatrix} 1/\chi_{nn} & 1/\chi_{np} \\ 1/\chi_{pn} & 1/\chi_{pp} \end{pmatrix}, \tag{6.1}$$

where the matrix elements $1/\chi_{ij}$ are given by

$$\frac{1}{\chi_{ij}} = \frac{\partial \mathcal{H}_i}{\partial \mathcal{M}_j} \qquad i, j = n, p. \tag{6.2}$$

Here $\mathcal{M}_j$ is the magnetization of the species $j$ per unit volume,

$$\mathcal{M}_j = \mu_j(\rho_{j\uparrow} - \rho_{j\downarrow}) = \mu_j \rho_j \Delta_j \,, \tag{6.3}$$

where $\mu_j$ is the magnetic moment of the species $j$,

$$\mu_n = -1.913\mu_N \,, \qquad \mu_p = 2.792\mu_N \,, \qquad \mu_N = \frac{e\hbar}{2m_p} = 0.105\, e\,\text{fm} \,, \tag{6.4}$$

and $\mathcal{H}_i$ is the magnetic field induced by the magnetization of the species $i$, which can be obtained from

$$\mathcal{H}_i = \rho \frac{\partial e}{\partial \mathcal{M}_i} \,, \tag{6.5}$$

where $e = e(\rho, \beta, \Delta_n, \Delta_p)$ is the total energy per particle.

Using Eqs. (6.3) and (6.5), the matrix elements $1/\chi_{ij}$[1] can be written as

$$\frac{1}{\chi_{ij}} = \frac{\rho}{\mu_i \rho_i \mu_j \rho_j} \frac{\partial^2 e}{\partial \Delta_i \partial \Delta_j} \,, \tag{6.6}$$

where the second derivatives can be taken at $\Delta_i = \Delta_j = 0$ if the field is assumed to be small.

The stability of matter against spin fluctuations is guaranteed if $\det(1/\chi) > 0$. A change of sign of the determinant indicates the existence of a spin instability and the onset of a phase transition towards a new spin ordering. It is convenient in order to highlight the role of the nucleon-nucleon interaction to study the magnetic susceptibility of the system in terms of the ratio $\det(1/\chi)/\det(1/\chi_F)$, where $\chi_F$ is the magnetic susceptibility of the two component free Fermi gas,

$$\frac{1}{\chi_F} = \frac{\rho}{\mu_i \rho_i \mu_j \rho_j} \frac{\partial^2 e_F}{\partial \Delta_i \partial \Delta_j} \,, \tag{6.7}$$

where the free Fermi gas energy per particle ($e_F$) is equal to the kinetic energy per particle, see (3.5). Thus, the two components read

$$\begin{aligned} \frac{1}{\chi_{Fnn}} &= \frac{\rho}{\mu_n^2 \rho_n^2} \frac{10}{9} \frac{\hbar^2 \xi}{2 m_n \rho} (1+\beta)^{5/3} \left[ (1+\Delta_n)^{-1/3} + (1-\Delta_p)^{-1/3} \right] , \\ \frac{1}{\chi_{Fpp}} &= \frac{\rho}{\mu_p^2 \rho_p^2} \frac{10}{9} \frac{\hbar^2 \xi}{2 m_p \rho} (1+\beta)^{5/3} \left[ (1+\Delta_p)^{-1/3} + (1-\Delta_p)^{-1/3} \right] . \end{aligned} \tag{6.8}$$

Expressing the total energy per particle as the sum of the kinetic and potential energy per particle, one can write the ratio $\det(1/\chi)/\det(1/\chi_F)$ as follows:

$$\begin{aligned} \frac{\det(1/\chi)}{\det(1/\chi_F)} = & \left( 1 + \frac{\dfrac{\partial^2 (V/N)}{\partial^2 \Delta_n}}{\dfrac{\partial^2 (T/N)}{\partial^2 \Delta_n}} \right) \left( 1 + \frac{\dfrac{\partial^2 (V/N)}{\partial^2 \Delta_p}}{\dfrac{\partial^2 (T/N)}{\partial^2 \Delta_p}} \right) \\ & - \left( \frac{\dfrac{\partial^2 (V/N)}{\partial \Delta_n \partial \Delta_p}}{\dfrac{\partial^2 (T/N)}{\partial^2 \Delta_n}} \right) \left( \frac{\dfrac{\partial^2 (V/N)}{\partial \Delta_p \partial \Delta_n}}{\dfrac{\partial^2 (T/N)}{\partial^2 \Delta_p}} \right) . \end{aligned} \tag{6.9}$$

[1] Analytic expressions of the magnetic susceptibility matrix elements for the Skyrme interaction are reported in the appendix A.5.

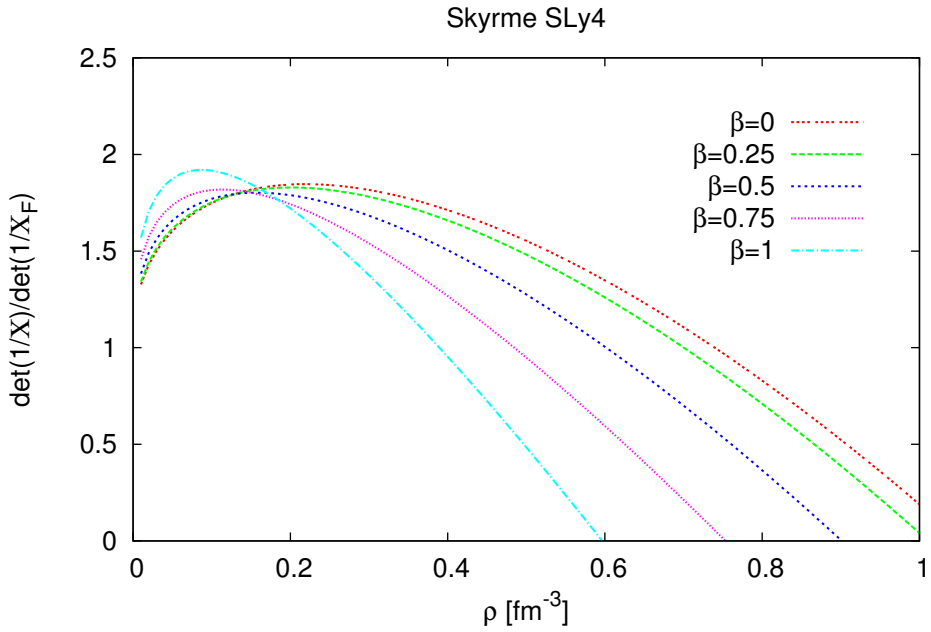


FIGURE 6.1: Ratio $\det(1/\chi)/\det(1/\chi_F)$ nuclear matter with different isospin asymmetries ($\beta = 0, 0.25, 0.5, 0.75, 1$) as a function of the total density for the Skyrme SLy4 interaction.

For neutron matter, the matrix (6.1) reduces to $1/\chi_{nn}$. Using the spin symmetry energy, see Eqs. (3.22) and (3.23), one can write down $1/\chi_{nn}$ as

$$\frac{1}{\chi_{nn}} = \frac{2\rho}{\mu_n^2 \rho_n^2} S_{sym}(\rho)\,, \tag{6.10}$$

which can be handy when the interaction is too complex to compute the derivatives.

In Fig. 6.1 we present the ratio $\det(1/\chi)/\det(1/\chi_F)$ of asymmetric nuclear matter with $\beta = 0, 0.25, 0.5, 0.75, 1$ as a function of the total density for the Skyrme SLy4 interaction. A phase transition appears at a critical density $\rho_c \sim 0.6\,\text{fm}^{-3}$ for neutron matter with the Skyrme SLy4 interaction. That is, for $\rho > 0.6\,\text{fm}^{-3}$ appears a spontaneous polarization of the ground state. As $\beta$ decreases, $\rho_t$ moves toward larger density values.

In Fig. 6.2 we compare the ratio $\det(1/\chi)/\det(1/\chi_F)$ of neutron matter as a function of the total density between the Skyrme SLy4 and the Gogny D1 interactions. We observe that, for densities $\rho < 0.1\,\text{fm}^{-3}$, the ratio $\det(1/\chi)/\det(1/\chi_F)$ for both the Skyrme SLy4 and Gogny D1 interactions present a similar behaviour. As density increases further away from $\rho = 0.1\,\text{fm}^{-3}$, the SLy4 ratio starts decreasing to eventually become negative at the critical density $\rho_c \sim 0.6\,\text{fm}^{-3}$, as we have already mentioned. Contrary, the D1 ratio keeps smoothly increasing with density thus, no spin instability is found at any density.

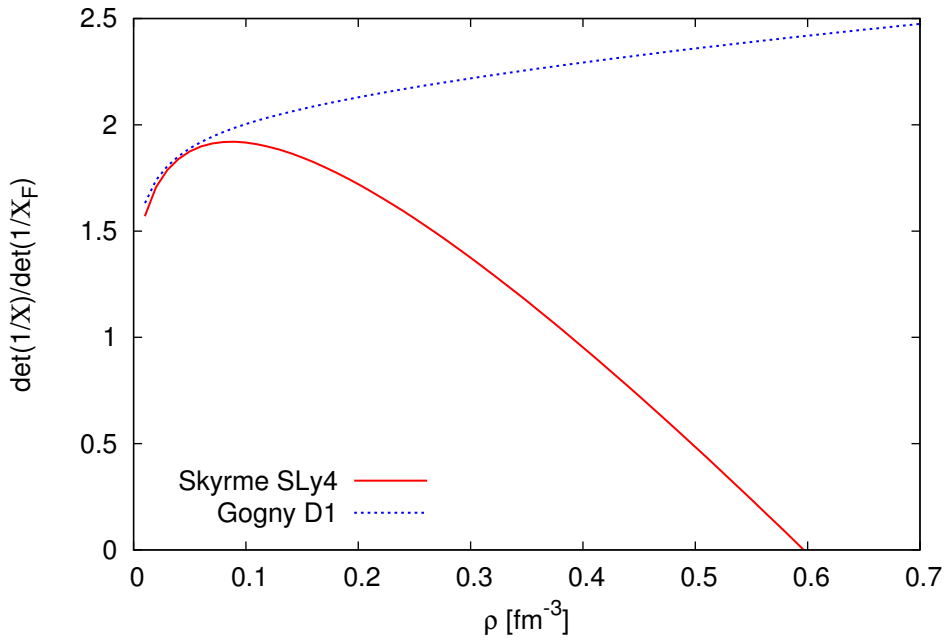


FIGURE 6.2: Ratio $\det(1/\chi)/\det(1/\chi_F)$ of neutron matter ($\beta = 1$) as a function of the total density for the Skyrme SLy4 interaction and the Gogny D1 interaction.

These results of pure neutron matter are consistent with the ones obtained for the spin symmetry energy (see subsection 3.3.2).

Notice that, for neutron matter, a change of sign on the spin symmetry energy approximation (3.23) is a sufficient condition for a phase transition, whereas a change of sign in the ratio $\det(1/\chi)/\det(1/\chi_F)$ is a necessary condition. That is why the densities at which the phase transition is predicted are different for the spin symmetry energy ($\rho_s \sim 0.72\,\text{fm}^{-3}$) and the magnetic susceptibility $\rho_c \sim 0.6\,\text{fm}^{-3}$.

# Summary and Conclusions

In this master thesis we have constructed the formalism to calculate the single-particle potential and energy per particle of homogeneous nuclear matter with any isospin asymmetry and spin polarization. The calculations have been performed in the framework of the Hartree-Fock formalism using effective interactions. We have considered the Skyrme SLy4 as an example of zero-range interactions and the original Gogny D1 as a characteristic finite-range force.

We have prepared a complete framework that allows the computation of: spin-isospin channel contributions, partial wave decompositions and calculations using the Slater function that permit to check the numerical calculations.

Once we have obtained the energy per particle, we have also considered the second derivatives of this energy with respect to isospin asymmetry to calculate the isospin symmetry energy, and with respect to the spin polarization to determinate the spin symmetry energy and study the magnetic susceptibility.

It has been found, in agreement with the existing literature, that the Skyrme SLy4, whose parametrization has incorporated microscopic results for neutron matter, does not show isospin instability and the symmetry energy is always positive, i.e., neutron matter never becomes the ground state. On the contrary, the symmetry energy for the Gogny interaction becomes zero at a density $\rho_s \sim 0.52\,\mathrm{fm}^{-3}$.

We have also checked that a parametrization of the energy per particle, previously suggested by Vidaña and Bombaci [31] for realistic interactions, adapts well to the effective interactions studied in the thesis, at least for small isospin asymmetries and spin polarizations. This parametrization allows us to express the energy per particle in terms of a few average matrix elements.

By computing the magnetic susceptibility, we have found that SLy4 predicts a spin instability at both neutron matter and asymmetric nuclear matter, with a critical density that shifts to smaller densities when increasing the isospin asymmetry. In the Gogny case, we have only performed the calculations for neutron matter and no sign of an instability has been found. Similar results, using other effective interactions, are found in the literature [46]. One should keep in mind that previous microscopic results [37, 31] do not show any spin instability. It would be useful to incorporate these results into the parametrization of the effective interactions [48].

Finally, we would like to extend this analysis to a wider family of Skyrme forces and the recent proposed Gogny forces. Also, we consider doing a similar analysis to explore the spinodal instabilities.

# Appendix A

# Integrals and Formulae

## A.1 Useful integrals

When solving the potential energy per particle, see Eq. (3.8), the integrals over momentum expressed in terms of a function $\Phi(\mathbf{k},\mathbf{k}')$ with a $k,k'$ dependence,

$$I[\Phi(\mathbf{k},\mathbf{k}');k_{F\sigma\tau},k'_{F\sigma'\tau'}] \equiv \frac{1}{2N}\frac{\Omega^2}{(2\pi)^6}\int_{k_{F\sigma\tau}}\int_{k'_{F\sigma'\tau'}} \mathrm{d}^3\mathbf{k}\,\mathrm{d}^3\mathbf{k}'\,\Phi(\mathbf{k},\mathbf{k}')\,, \tag{A.1}$$

where $\Omega$ is the volume of the system and $N$ the number of particles, result in Eqs. (A.2), (A.3) and (A.4) for the Skyrme interaction and in Eqs. (A.2) and (A.5) for the Gogny interaction.

$$I[\Omega^{-1};k_{F\sigma\tau},k'_{F\sigma'\tau'}] = \frac{1}{2N}\frac{\Omega}{(2\pi)^6}\left(\frac{4}{3}\pi {k_{F\sigma\tau}}^3\right)\left(\frac{4}{3}\pi {k'_{F\sigma'\tau'}}^3\right) = \frac{1}{2\rho}\rho_{\sigma\tau}\rho_{\sigma'\tau'}\,; \tag{A.2}$$

$$\begin{aligned} I[\Omega^{-1}(\mathbf{k}^2+\mathbf{k}'^2);k_{F\sigma\tau},k'_{F\sigma'\tau'}] &= \frac{1}{2N}\frac{\Omega}{(2\pi)^6}\left[\left(\frac{4}{3}\pi {k_{F\sigma\tau}}^3\right)\left(\frac{4}{5}\pi {k'_{F\sigma'\tau'}}^5\right)\right. \\ &\qquad \left. + \left(\frac{4}{3}\pi {k'_{F\sigma'\tau'}}^3\right)\left(\frac{4}{5}\pi {k_{F\sigma\tau}}^5\right)\right] \\ &= \frac{1}{2\rho}(\xi_{\sigma'\tau'}\rho_{\sigma\tau}+\xi_{\sigma\tau}\rho_{\sigma'\tau'})\,; \end{aligned} \tag{A.3}$$

$$I[\Omega^{-1}(\mathbf{k}\cdot\mathbf{k}');k_{F\sigma\tau},k_{F\sigma'\tau'}] = 0\,; \tag{A.4}$$

$$
\begin{aligned}
I\left[\Omega^{-1}e^{-\frac{\mu_i^2}{4}|\mathbf{k}-\mathbf{k}'|^2};k_{F\sigma\tau},k'_{F\sigma'\tau'}\right] &= \\
&= \frac{1}{2\rho}\frac{1}{2\pi^2\mu_i^3}\frac{1}{3\pi^2\mu_i^3} \\
&\times \Big[\big(\mu_i^2{k_{F\sigma\tau}}^2-\mu_i k_{F\sigma\tau}\mu_i k'_{F\sigma'\tau'}+\mu_i^2{k'_{F\sigma'\tau'}}^2-2\big)e^{-\frac{\mu_i^2}{4}(k_{F\sigma\tau}+k'_{F\sigma'\tau'})^2} \\
&- \big(\mu_i^2{k_{F\sigma\tau}}^2+\mu_i k_{F\sigma\tau}\mu_i k'_{F\sigma'\tau'}+\mu_i^2{k'_{F\sigma'\tau'}}^2-2\big)e^{-\frac{\mu_i^2}{4}(k_{F\sigma\tau}-k'_{F\sigma'\tau'})^2} \\
&- \frac{\sqrt{\pi}\mu_i^3}{2}\big({k_{F\sigma\tau}}^3-{k'_{F\sigma'\tau'}}^3\big)\,\mathrm{erf}\left(\frac{\mu_i}{2}(k_{F\sigma\tau}-k'_{F\sigma'\tau'})\right) \\
&+ \frac{\sqrt{\pi}\mu_i^3}{2}\big({k_{F\sigma\tau}}^3+{k'_{F\sigma'\tau'}}^3\big)\,\mathrm{erf}\left(\frac{\mu_i}{2}(k_{F\sigma\tau}+k'_{F\sigma'\tau'})\right)\Big] \\
&= \frac{1}{4\rho\pi^2\mu_i^3}g(k_{F\sigma\tau},k'_{F\sigma'\tau'})\,.
\end{aligned}
\tag{A.5}
$$

The single-component density $\rho_{\sigma\tau}$ is related with the single-component Fermi momentum $k_{F\sigma\tau}$ by Eq. (2.16):

$$
\rho_{\sigma\tau}=\frac{{k_{F\sigma\tau}}^3}{6\pi^2}\,,\qquad k_{F\sigma\tau}=\big(6\pi^2\rho_{\sigma\tau}\big)^{1/3}\,. \tag{A.6}
$$

$\xi_{\tau\sigma}$ are related to the average kinetic energy of the Fermi model of nuclear matter [22], expressed in Eq. (3.6):

$$
\begin{aligned}
\xi_{\tau\sigma} &= \frac{3}{5}k_{F\sigma\tau}^2\rho_{\tau\sigma}=\frac{3}{5}(6\pi^2\rho_{\tau\sigma})^{2/3}\rho_{\tau\sigma} \\
&= \frac{3}{20}\left(\frac{3}{2}\pi^2\rho\right)^{2/3}\rho(1\pm\beta)^{5/3}(1\pm\Delta_\tau)^{5/3}\,.
\end{aligned}
\tag{A.7}
$$

$g_i(k_{F\sigma\tau},k'_{F\sigma'\tau'})$ is given in Eq. (3.12) by:

$$
\begin{aligned}
g_i(k_{F\sigma\tau},k'_{F\sigma'\tau'}) = \frac{1}{3\pi^2\mu_i^3}\Big[&\big(\mu_i^2k_{F\sigma\tau}^2-\mu_i k_{F\sigma\tau}\mu_i k'_{F\sigma'\tau'}+\mu_i^2k'^2_{F\sigma'\tau'}-2\big)e^{-\frac{\mu_i^2}{4}(k_{F\sigma\tau}+k'_{F\sigma'\tau'})^2} \\
&- \big(\mu_i^2k_{F\sigma\tau}^2+\mu_i k_{F\sigma\tau}\mu_i k'_{F\sigma'\tau'}+\mu_i^2k'^2_{F\sigma'\tau'}-2\big)e^{-\frac{\mu_i^2}{4}(k_{F\sigma\tau}-k'_{F\sigma'\tau'})^2} \\
&- \frac{\sqrt{\pi}\mu_i^3}{2}\big(k_{F\sigma\tau}^3-k'^3_{F\sigma'\tau'}\big)\,\mathrm{erf}\left(\frac{\mu_i}{2}(k_{F\sigma\tau}-k'_{F\sigma'\tau'})\right) \\
&+ \frac{\sqrt{\pi}\mu_i^3}{2}\big(k_{F\sigma\tau}^3+k'^3_{F\sigma'\tau'}\big)\,\mathrm{erf}\left(\frac{\mu_i}{2}(k_{F\sigma\tau}+k'_{F\sigma'\tau'})\right)\Big]\,.
\end{aligned}
\tag{A.8}
$$

Notice that $g_i(k_{F\sigma\tau},0)=g_i(0,k'_{F\sigma'\tau'})=g_i(0,0)=0$.

## A.2 Skyrme kinetic and potential energy

For a more convenient notation, we define

$$\xi = \frac{3}{20}\left(\frac{3}{2}\pi^2\rho\right)^{2/3}\rho\,, \tag{A.9}$$

from Eq. (A.7).

Using Eqs. (2.1), (2.2) and (2.3), we write down the kinetic energy per particle as a function of $\rho, \beta, \Delta_n$ and $\Delta_p$:

$$\begin{aligned}\frac{\langle T\rangle}{N} &= \frac{\hbar^2\xi}{2m_n\rho}(1+\beta)^{5/3}\left[(1+\Delta_n)^{5/3}+(1-\Delta_n)^{5/3}\right] \\ &+ \frac{\hbar^2\xi}{2m_p\rho}(1-\beta)^{5/3}\left[(1+\Delta_p)^{5/3}+(1-\Delta_p)^{5/3}\right].\end{aligned} \tag{A.10}$$

The same goes for the Skyrme potential energy per particle:

$$
\begin{aligned}
\frac{\langle V^{\mathrm{Sk}}\rangle}{N} = {} & \frac{\xi}{16}[2t_2(1+x_2)]\Big[(1+\beta)^{8/3}\Big\{(1+\Delta_n)^{8/3}+(1-\Delta_n)^{8/3}\Big\} \\
& \qquad + (1-\beta)^{8/3}\Big\{(1+\Delta_p)^{8/3}+(1-\Delta_p)^{8/3}\Big\}\Big] \\
& + \frac{\xi}{16}[t_1(1-x_1)+t_2(1+x_2)]\Big[(1+\beta)^{8/3}\Big\{(1+\Delta_n)^{5/3}(1-\Delta_n) \\
& \qquad + (1-\Delta_n)^{5/3}(1+\Delta_n)\Big\} \\
& \qquad + (1-\beta)^{8/3}\Big\{(1+\Delta_p)^{5/3}(1-\Delta_p) \\
& \qquad + (1-\Delta_p)^{5/3}(1+\Delta_p)\Big\}\Big] \\
& + \frac{\xi}{16}[t_1(1+x_1)+t_2(1+x_2)] \\
& \times \Big[(1+\beta)^{5/3}(1-\beta)\Big\{(1+\Delta_n)^{5/3}(1+\Delta_p)+(1-\Delta_n)^{5/3}(1-\Delta_p)\Big\} \\
& \quad + (1-\beta)^{5/3}(1+\beta)\Big\{(1+\Delta_p)^{5/3}(1+\Delta_n)+(1-\Delta_p)^{5/3}(1-\Delta_n)\Big\}\Big] \\
& + \frac{\xi}{16}[t_1+t_2] \\
& \times \Big[(1+\beta)^{5/3}(1-\beta)\Big\{(1+\Delta_n)^{5/3}(1-\Delta_p)+(1-\Delta_n)^{5/3}(1+\Delta_p)\Big\} \\
& \quad + (1-\beta)^{5/3}(1+\beta)\Big\{(1+\Delta_p)^{5/3}(1-\Delta_n)+(1-\Delta_p)^{5/3}(1+\Delta_n)\Big\}\Big] \\
& + \frac{\rho}{4}\Big[t_0+\frac{1}{6}t_3\rho^{\gamma}\Big]\big(1-\beta^2\big) \\
& + \frac{\rho}{16}\Big[t_0x_0+\frac{1}{6}t_3x_3\rho^{\gamma}\Big]\big(1-\beta^2\big)[(1+\Delta_n)(1+\Delta_p)+(1-\Delta_n)(1-\Delta_p)] \\
& + \frac{\rho}{16}\Big[t_0(1-x_0)+\frac{1}{6}t_3(1-x_3)\rho^{\gamma}\Big]\big[(1+\beta)^2(1-\Delta_n^2)+(1-\beta)^2(1-\Delta_p^2)\big]
\end{aligned}
\tag{A.11}
$$

## A.3 Slater results for the Gogny interaction

The potential energy per particle expressed in terms of the Slater function, see Eq. (3.16), results in the following expressions for the Gogny interaction:

- Non-polarized nuclear matter:

$$\frac{\langle V^{\mathrm{G}}\rangle}{N} = \frac{3}{8}t_0\rho^{\gamma+1} + \frac{\rho}{2}\frac{1}{\nu_\sigma^2\nu_\tau^2}\int \mathrm{d}^3\mathbf{r}\,\hat{v}(\mathbf{r}) \times \sum_{\sigma\sigma'\tau\tau'}\left[\left(W_i + \frac{1}{2}B_i - \frac{1}{2}H_i - \frac{1}{4}M_i\right) - \left(\frac{1}{4}W_i + \frac{1}{2}B_i - \frac{1}{2}H_i - M_i\right)\ell^2(k_F r)\right]; \tag{A.12}$$

- Polarized nuclear matter:

$$\frac{\langle V^{\mathrm{G}}\rangle}{N} = \frac{1}{2}t_0(1+x_0)\rho^{\gamma+1} + \frac{\rho}{2}\frac{1}{\nu_\sigma^2\nu_\tau^2}\int \mathrm{d}^3\mathbf{r}\,\hat{v}(\mathbf{r}) \times \sum_{\sigma\sigma'\tau\tau'}\left[\left(W_i + B_i - \frac{1}{2}H_i - \frac{1}{2}M_i\right) - \left(\frac{1}{2}W_i + \frac{1}{2}B_i - H_i - M_i\right)\ell^2(k_F r)\right]; \tag{A.13}$$

- Anti-polarized nuclear matter:

$$\frac{\langle V^{\mathrm{G}}\rangle}{N} = \frac{1}{4}t_0x_0\rho^{\gamma+1} + \frac{\rho}{2}\frac{1}{\nu_\sigma^2\nu_\tau^2}\int \mathrm{d}^3\mathbf{r}\,\hat{v}(\mathbf{r}) \times \sum_{\sigma\sigma'\tau\tau'}\left[\left(W_i + \frac{1}{2}B_i - \frac{1}{8}H_i - \frac{1}{2}M_i\right) - \left(\frac{1}{2}W_i + \frac{1}{8}B_i - \frac{1}{2}H_i - M_i\right)\ell^2(k_F r)\right]; \tag{A.14}$$

- Non-polarized neutron matter:

$$\frac{\langle V^{\mathrm{G}}\rangle}{N} = \frac{\rho}{2}\frac{1}{\nu_\sigma^2\nu_\tau^2}\int \mathrm{d}^3\mathbf{r}\,\hat{v}(\mathbf{r}) \times \sum_{\sigma\sigma'\tau\tau'}\left[\left(W_i + \frac{1}{2}B_i - H_i - \frac{1}{2}M_i\right) - \left(\frac{1}{2}W_i + B_i - \frac{1}{2}H_i - M_i\right)\ell^2(k_F r)\right]; \tag{A.15}$$

- Polarized neutron matter:

$$\frac{\langle V^{\mathrm{G}}\rangle}{N} = \frac{\rho}{2}\frac{1}{\nu_\sigma^2\nu_\tau^2}\int \mathrm{d}^3\mathbf{r}\,\hat{v}(\mathbf{r}) \sum_{\sigma\sigma'\tau\tau'}\left[(W_i + B_i - H_i - M_i)(1 - \ell^2(k_F r))\right]. \tag{A.16}$$

## A.4 Spin-isospin third component channel contributions

There are a total of 16 contributions of the spin-isospin ($S$, $T$) third component ($M_S$, $M_T$) channels to the potential energy per particle. All of them are provided below for both the Skyrme and Gogny interactions.

For the Skyrme interaction, the $\left\langle V^{\text{Sk}}_{STM_SM_T}\right\rangle/N$ contributions read

$$\frac{\left\langle V^{\text{Sk}}_{1111}\right\rangle}{N} = \frac{1}{4\rho}[2t_2(1+x_2)]\xi_{p\uparrow}\rho_{p\uparrow}\,; \tag{A.17}$$

$$\frac{\left\langle V^{\text{Sk}}_{1110}\right\rangle}{N} = \frac{1}{2}\left\{\frac{1}{4\rho}[2t_2(1+x_2)](\xi_{n\uparrow}\rho_{p\uparrow}+\xi_{p\uparrow}\rho_{n\uparrow})\right\}; \tag{A.18}$$

$$\frac{\left\langle V^{\text{Sk}}_{111-1}\right\rangle}{N} = \frac{1}{4\rho}[2t_2(1+x_2)]\xi_{n\uparrow}\rho_{n\uparrow}\,; \tag{A.19}$$

$$\frac{\left\langle V^{\text{Sk}}_{1101}\right\rangle}{N} = \frac{1}{2}\left\{\frac{1}{4\rho}[2t_2(1+x_2)](\xi_{p\uparrow}\rho_{p\downarrow}+\xi_{p\downarrow}\rho_{p\uparrow})\right\}; \tag{A.20}$$

$$\frac{\left\langle V^{\text{Sk}}_{1100}\right\rangle}{N} = \frac{1}{4}\left\{\frac{1}{4\rho}[2t_2(1+x_2)](\xi_{n\uparrow}\rho_{p\downarrow}+\xi_{n\downarrow}\rho_{p\uparrow}+\xi_{p\uparrow}\rho_{n\downarrow}+\xi_{p\downarrow}\rho_{n\uparrow})\right\}; \tag{A.21}$$

$$\frac{\left\langle V^{\text{Sk}}_{110-1}\right\rangle}{N} = \frac{1}{2}\left\{\frac{1}{4\rho}[2t_2(1+x_2)](\xi_{n\uparrow}\rho_{n\downarrow}+\xi_{n\downarrow}\rho_{n\uparrow})\right\}; \tag{A.22}$$

$$\frac{\left\langle V^{\text{Sk}}_{11-11}\right\rangle}{N} = \frac{1}{4\rho}[2t_2(1+x_2)]\xi_{p\downarrow}\rho_{p\downarrow}\,; \tag{A.23}$$

$$\frac{\left\langle V^{\text{Sk}}_{11-10}\right\rangle}{N} = \frac{1}{2}\left\{\frac{1}{4\rho}[2t_2(1+x_2)](\xi_{n\downarrow}\rho_{p\downarrow}+\xi_{p\downarrow}\rho_{n\downarrow})\right\}; \tag{A.24}$$

$$\frac{\left\langle V^{\text{Sk}}_{11-1-1}\right\rangle}{N} = \frac{1}{4\rho}[2t_2(1+x_2)]\xi_{n\downarrow}\rho_{n\downarrow}\,; \tag{A.25}$$

$$\frac{\left\langle V^{\mathrm{Sk}}_{1010}\right\rangle}{N} = \frac{1}{2}\Bigg\{\frac{2}{\rho}\left[t_0(1+x_0)+\frac{1}{6}t_3(1+x_3)\rho^{\gamma}\right]\rho_{n\uparrow}\rho_{p\uparrow} + \frac{1}{4\rho}[2t_1(1+x_1)]\left(\xi_{n\uparrow}\rho_{p\uparrow}+\xi_{p\uparrow}\rho_{n\uparrow}\right)\Bigg\}; \tag{A.26}$$

$$\frac{\left\langle V^{\mathrm{Sk}}_{1000}\right\rangle}{N} = \frac{1}{4}\Bigg\{\frac{2}{\rho}\left[t_0(1+x_0)+\frac{1}{6}t_3(1+x_3)\rho^{\gamma}\right]\left(\rho_{n\uparrow}\rho_{p\downarrow}+\rho_{n\downarrow}\rho_{p\uparrow}\right) + \frac{1}{4\rho}[2t_1(1+x_1)]\left(\xi_{n\uparrow}\rho_{p\downarrow}+\xi_{n\downarrow}\rho_{p\uparrow}+\xi_{p\uparrow}\rho_{n\downarrow}+\xi_{p\downarrow}\rho_{n\uparrow}\right)\Bigg\}; \tag{A.27}$$

$$\frac{\left\langle V^{\mathrm{Sk}}_{10-10}\right\rangle}{N} = \frac{1}{2}\Bigg\{\frac{2}{\rho}\left[t_0(1+x_0)+\frac{1}{6}t_3(1+x_3)\rho^{\gamma}\right]\rho_{n\downarrow}\rho_{p\downarrow} + \frac{1}{4\rho}[2t_1(1+x_1)]\left(\xi_{n\downarrow}\rho_{p\downarrow}+\xi_{p\downarrow}\rho_{n\downarrow}\right)\Bigg\}; \tag{A.28}$$

$$\frac{\left\langle V^{\mathrm{Sk}}_{0101}\right\rangle}{N} = \frac{1}{2}\Bigg\{\frac{2}{\rho}\left[t_0(1-x_0)+\frac{1}{6}t_3(1-x_3)\rho^{\gamma}\right]\rho_{p\uparrow}\rho_{p\downarrow} + \frac{1}{4\rho}[2t_1(1-x_1)]\left(\xi_{p\uparrow}\rho_{p\downarrow}+\xi_{p\downarrow}\rho_{p\uparrow}\right)\Bigg\}; \tag{A.29}$$

$$\frac{\left\langle V^{\mathrm{Sk}}_{0100}\right\rangle}{N} = \frac{1}{4}\Bigg\{\frac{2}{\rho}\left[t_0(1-x_0)+\frac{1}{6}t_3(1-x_3)\rho^{\gamma}\right]\left(\rho_{n\uparrow}\rho_{p\downarrow}+\rho_{n\downarrow}\rho_{p\uparrow}\right) + \frac{1}{4\rho}[2t_1(1-x_1)]\left(\xi_{n\uparrow}\rho_{p\downarrow}+\xi_{n\downarrow}\rho_{p\uparrow}+\xi_{p\uparrow}\rho_{n\downarrow}+\xi_{p\downarrow}\rho_{n\uparrow}\right)\Bigg\}; \tag{A.30}$$

$$\frac{\left\langle V^{\mathrm{Sk}}_{010-1}\right\rangle}{N} = \frac{1}{2}\Bigg\{\frac{2}{\rho}\left[t_0(1-x_0)+\frac{1}{6}t_3(1-x_3)\rho^{\gamma}\right]\rho_{n\uparrow}\rho_{n\downarrow} + \frac{1}{4\rho}[2t_1(1-x_1)]\left(\xi_{n\uparrow}\rho_{n\downarrow}+\xi_{n\downarrow}\rho_{n\uparrow}\right)\Bigg\}; \tag{A.31}$$

$$\frac{\left\langle V^{\mathrm{Sk}}_{0000}\right\rangle}{N} = \frac{1}{4}\Bigg\{\frac{1}{4\rho}[2t_2(1-x_2)]\left(\xi_{n\uparrow}\rho_{p\downarrow}+\xi_{n\downarrow}\rho_{p\uparrow}+\xi_{p\uparrow}\rho_{n\downarrow}+\xi_{p\downarrow}\rho_{n\uparrow}\right)\Bigg\}; \tag{A.32}$$

For the Gogny interaction, the $\left\langle V^{\mathrm{G}}_{STM_SM_T}\right\rangle/N$ contributions read

$$\frac{\left\langle V^{\mathrm{G}}_{1111}\right\rangle}{N} = \frac{\pi^{3/2}}{2\rho}\sum_i \mu_i^3[W_i+B_i-H_i-M_i]\rho^2_{p\uparrow} - \frac{1}{4\rho\sqrt{\pi}}\sum_i [W_i+B_i-H_i-M_i]g_i(k_{Fp\uparrow},k_{Fp\uparrow})\,; \tag{A.33}$$

$$\frac{\left\langle V^{\mathrm{G}}_{1110}\right\rangle}{N} = \frac{\pi^{3/2}}{2\rho}\sum_i \mu_i^3[W_i+B_i-H_i-M_i]\rho_{n\uparrow}\rho_{p\uparrow} - \frac{1}{2}\frac{1}{4\rho\sqrt{\pi}}\sum_i [W_i+B_i-H_i-M_i]\Big(g_i(k_{Fn\uparrow},k_{Fp\uparrow})+g_i(k_{Fp\uparrow},k_{Fn\uparrow})\Big)\,; \tag{A.34}$$

$$\frac{\left\langle V^{\mathrm{G}}_{111-1}\right\rangle}{N} = \frac{\pi^{3/2}}{2\rho}\sum_i \mu_i^3[W_i+B_i-H_i-M_i]\rho^2_{n\uparrow} - \frac{1}{4\rho\sqrt{\pi}}\sum_i [W_i+B_i-H_i-M_i]g_i(k_{Fn\uparrow},k_{Fn\uparrow})\,; \tag{A.35}$$

$$\frac{\left\langle V^{\mathrm{G}}_{1101}\right\rangle}{N} = \frac{\pi^{3/2}}{2\rho}\sum_i \mu_i^3[W_i+B_i-H_i-M_i]\rho_{p\uparrow}\rho_{p\downarrow} - \frac{1}{2}\frac{1}{4\rho\sqrt{\pi}}\sum_i [W_i+B_i-H_i-M_i]\Big(g_i(k_{Fp\uparrow},k_{Fp\downarrow})+g_i(k_{Fp\downarrow},k_{Fp\uparrow})\Big)\,; \tag{A.36}$$

$$\frac{\left\langle V^{\mathrm{G}}_{1100}\right\rangle}{N} = \frac{1}{2}\frac{\pi^{3/2}}{2\rho}\sum_i \mu_i^3[W_i+B_i-H_i-M_i](\rho_{n\uparrow}\rho_{p\downarrow}+\rho_{n\downarrow}\rho_{p\uparrow}) - \frac{1}{4}\frac{1}{4\rho\sqrt{\pi}}\sum_i [W_i+B_i-H_i-M_i]\Big(g_i(k_{Fn\uparrow},k_{Fp\downarrow})+g_i(k_{Fn\downarrow},k_{Fp\uparrow}) + g_i(k_{Fp\uparrow},k_{Fn\downarrow})+g_i(k_{Fp\downarrow},k_{Fn\uparrow})\Big)\,; \tag{A.37}$$

$$\frac{\left\langle V^{\mathrm{G}}_{110-1}\right\rangle}{N} = \frac{\pi^{3/2}}{2\rho}\sum_i \mu_i^3[W_i+B_i-H_i-M_i]\rho_{n\uparrow}\rho_{n\downarrow} - \frac{1}{2}\frac{1}{4\rho\sqrt{\pi}}\sum_i [W_i+B_i-H_i-M_i]\Big(g_i(k_{Fn\uparrow},k_{Fn\downarrow})+g_i(k_{Fn\downarrow},k_{Fn\uparrow})\Big)\,; \tag{A.38}$$

$$\frac{\left\langle V^{\rm G}_{11-11}\right\rangle}{N} = \frac{\pi^{3/2}}{2\rho}\sum_i \mu_i^3[W_i + B_i - H_i - M_i]\rho^2_{p\downarrow} - \frac{1}{4\rho\sqrt{\pi}}\sum_i [W_i + B_i - H_i - M_i] g_i(k_{Fp\downarrow}, k_{Fp\downarrow})\,; \tag{A.39}$$

$$\frac{\left\langle V^{\rm G}_{11-10}\right\rangle}{N} = \frac{\pi^{3/2}}{2\rho}\sum_i \mu_i^3[W_i + B_i - H_i - M_i]\rho_{n\downarrow}\rho_{p\downarrow} - \frac{1}{2}\frac{1}{4\rho\sqrt{\pi}}\sum_i [W_i + B_i - H_i - M_i]\Big(g_i(k_{Fn\downarrow}, k_{Fp\downarrow}) + g_i(k_{Fp\downarrow}, k_{Fn\downarrow})\Big)\,; \tag{A.40}$$

$$\frac{\left\langle V^{\rm G}_{11-1-1}\right\rangle}{N} = \frac{\pi^{3/2}}{2\rho}\sum_i \mu_i^3[W_i + B_i - H_i - M_i]\rho^2_{n\downarrow} - \frac{1}{4\rho\sqrt{\pi}}\sum_i [W_i + B_i - H_i - M_i] g_i(k_{Fn\downarrow}, k_{Fn\downarrow})\,; \tag{A.41}$$

$$\frac{\left\langle V^{\rm G}_{1010}\right\rangle}{N} = \rho^{\gamma-1}t_0[1 + x_0]\rho_{n\uparrow}\rho_{p\uparrow} + \frac{\pi^{3/2}}{2\rho}\sum_i \mu_i^3[W_i + B_i + H_i + M_i]\rho_{n\uparrow}\rho_{p\uparrow} - \frac{1}{2}\frac{1}{4\rho\sqrt{\pi}}\sum_i [-W_i - B_i - H_i - M_i]\Big(g_i(k_{Fn\uparrow}, k_{Fp\uparrow}) + g_i(k_{Fp\uparrow}, k_{Fn\uparrow})\Big)\,; \tag{A.42}$$

$$\frac{\left\langle V^{\rm G}_{1000}\right\rangle}{N} = \frac{1}{2}\rho^{\gamma-1}t_0[1 + x_0](\rho_{n\uparrow}\rho_{p\downarrow} + \rho_{n\downarrow}\rho_{p\uparrow}) + \frac{1}{2}\frac{\pi^{3/2}}{2\rho}\sum_i \mu_i^3[W_i + B_i + H_i + M_i](\rho_{n\uparrow}\rho_{p\downarrow} + \rho_{n\downarrow}\rho_{p\uparrow}) - \frac{1}{4}\frac{1}{4\rho\sqrt{\pi}}\sum_i [-W_i - B_i - H_i - M_i]\Big(g_i(k_{Fn\uparrow}, k_{Fp\downarrow}) + g_i(k_{Fn\downarrow}, k_{Fp\uparrow}) + g_i(k_{Fp\uparrow}, k_{Fn\downarrow}) + g_i(k_{Fp\downarrow}, k_{Fn\uparrow})\Big)\,; \tag{A.43}$$

$$\begin{aligned}\frac{\left\langle V^{\mathrm{G}}_{10-10}\right\rangle}{N} &= \rho^{\gamma-1}t_0[1+x_0]\rho_{n\downarrow}\rho_{p\downarrow}\\ &+\frac{\pi^{3/2}}{2\rho}\sum_i \mu_i^3[W_i+B_i+H_i+M_i]\rho_{n\downarrow}\rho_{p\downarrow}\\ &-\frac{1}{2}\frac{1}{4\rho\sqrt{\pi}}\sum_i[-W_i-B_i-H_i-M_i]\Big(g_i(k_{Fn\downarrow},k_{Fp\downarrow})+g_i(k_{Fp\downarrow},k_{Fn\downarrow})\Big);\end{aligned} \tag{A.44}$$

$$\begin{aligned}\frac{\left\langle V^{\mathrm{G}}_{0101}\right\rangle}{N} &= \rho^{\gamma-1}t_0[1-x_0]\rho_{p\uparrow}\rho_{p\downarrow}\\ &+\frac{\pi^{3/2}}{2\rho}\sum_i \mu_i^3[W_i-B_i-H_i+M_i]\rho_{p\uparrow}\rho_{p\downarrow}\\ &-\frac{1}{2}\frac{1}{4\rho\sqrt{\pi}}\sum_i[-W_i+B_i+H_i-M_i]\Big(g_i(k_{Fp\uparrow},k_{Fp\downarrow})+g_i(k_{Fp\downarrow},k_{Fp\uparrow})\Big);\end{aligned} \tag{A.45}$$

$$\begin{aligned}\frac{\left\langle V^{\mathrm{G}}_{0100}\right\rangle}{N} &= \frac{1}{2}\rho^{\gamma-1}t_0[1-x_0](\rho_{n\uparrow}\rho_{p\downarrow}+\rho_{n\downarrow}\rho_{p\uparrow})\\ &+\frac{1}{2}\frac{\pi^{3/2}}{2\rho}\sum_i \mu_i^3[W_i-B_i-H_i+M_i](\rho_{n\uparrow}\rho_{p\downarrow}+\rho_{n\downarrow}\rho_{p\uparrow})\\ &-\frac{1}{4}\frac{1}{4\rho\sqrt{\pi}}\sum_i[-W_i+B_i+H_i-M_i]\Big(g_i(k_{Fn\uparrow},k_{Fp\downarrow})+g_i(k_{Fn\downarrow},k_{Fp\uparrow})\\ &\qquad+g_i(k_{Fp\uparrow},k_{Fn\downarrow})+g_i(k_{Fp\downarrow},k_{Fn\uparrow})\Big);\end{aligned} \tag{A.46}$$

$$\begin{aligned}\frac{\left\langle V^{\mathrm{G}}_{010-1}\right\rangle}{N} &= \rho^{\gamma-1}t_0[1-x_0]\rho_{n\uparrow}\rho_{n\downarrow}\\ &+\frac{\pi^{3/2}}{2\rho}\sum_i \mu_i^3[W_i-B_i-H_i+M_i]\rho_{n\uparrow}\rho_{n\downarrow}\\ &-\frac{1}{2}\frac{1}{4\rho\sqrt{\pi}}\sum_i[-W_i+B_i+H_i-M_i]\Big(g_i(k_{Fn\uparrow},k_{Fn\downarrow})+g_i(k_{Fn\downarrow},k_{Fn\uparrow})\Big);\end{aligned} \tag{A.47}$$

$$\frac{\left\langle V^{\mathrm{G}}_{0000}\right\rangle}{N} = \frac{1}{2}\frac{\pi^{3/2}}{2\rho}\sum_i \mu_i^3[W_i - B_i + H_i - M_i](\rho_{n\uparrow}\rho_{p\downarrow} + \rho_{n\downarrow}\rho_{p\uparrow}) - \frac{1}{4}\frac{1}{4\rho\sqrt{\pi}}\sum_i [W_i - B_i + H_i - M_i]\Big(g_i(k_{Fn\uparrow}, k_{Fp\downarrow}) + g_i(k_{Fn\downarrow}, k_{Fp\uparrow}) + g_i(k_{Fp\uparrow}, k_{Fn\downarrow}) + g_i(k_{Fp\downarrow}, k_{Fn\uparrow})\Big); \tag{A.48}$$

## A.5 Magnetic susceptibility matrix elements for the Skyrme interaction

Analytic expressions of the Skyrme interaction magnetic susceptibility matrix elements, see Eq. (6.6), are pesented below:

$$\begin{aligned}\frac{1}{\chi_{nn}} = \frac{\rho}{\mu_n^2\rho_n^2}\Bigg\{ & \frac{10}{9}\frac{\hbar^2\xi}{2m_n\rho}(1+\beta)^{5/3}\left[(1+\Delta_n)^{-1/3} + (1-\Delta_n)^{-1/3}\right] \\ & + \frac{\xi}{16}\frac{40}{9}[2t_2(1+x_2)](1+\beta)^{8/3}\left[(1+\Delta_n)^{2/3} + (1-\Delta_n)^{2/3}\right] \\ & + \frac{\xi}{16}\frac{10}{9}[t_1(1-x_1) + t_2(1+x_2)] \\ & \times (1+\beta)^{8/3}\Big[(1+\Delta_n)^{-1/3}(1-\Delta_n) - 3(1+\Delta_n)^{2/3} \\ & \qquad + (1-\Delta_n)^{-1/3}(1+\Delta_n) - 3(1-\Delta_n)^{2/3}\Big] \\ & + \frac{\xi}{16}\frac{10}{9}[t_1(1+x_1) + t_2(1+x_2)] \\ & \times (1+\beta)^{5/3}(1-\beta)\left[(1+\Delta_n)^{-1/3}(1+\Delta_p) + (1-\Delta_n)^{-1/3}(1-\Delta_p)\right] \\ & + \frac{\xi}{16}\frac{10}{9}[t_1 + t_2] \\ & \times (1+\beta)^{5/3}(1-\beta)\left[(1+\Delta_n)^{-1/3}(1-\Delta_p) + (1-\Delta_n)^{-1/3}(1+\Delta_p)\right] \\ & - \frac{2\rho}{16}\left[t_0(1-x_0) + \frac{1}{6}t_3(1-x_3)\rho^\gamma\right](1+\beta)^2\Bigg\}; \end{aligned} \tag{A.49}$$

$$\begin{aligned}\frac{1}{\chi_{pp}} = \frac{\rho}{\mu_p^2\rho_p^2}\Bigg\{ & \frac{10}{9}\frac{\hbar^2\xi}{2m_p\rho}(1-\beta)^{5/3}\big[(1+\Delta_p)^{-1/3}+(1-\Delta_p)^{-1/3}\big] \\ & + \frac{\xi}{16}\frac{40}{9}[2t_2(1+x_2)](1-\beta)^{8/3}\big[(1+\Delta_p)^{2/3}+(1-\Delta_p)^{2/3}\big] \\ & + \frac{\xi}{16}\frac{10}{9}[t_1(1-x_1)+t_2(1+x_2)] \\ & \times (1-\beta)^{8/3}\Big[(1+\Delta_p)^{-1/3}(1-\Delta_p) - 3(1+\Delta_p)^{2/3} \\ & \qquad + (1-\Delta_p)^{-1/3}(1+\Delta_p) - 3(1-\Delta_p)^{2/3}\Big] \\ & + \frac{\xi}{16}\frac{10}{9}[t_1(1+x_1)+t_2(1+x_2)] \\ & \times (1-\beta)^{5/3}(1+\beta)\big[(1+\Delta_p)^{-1/3}(1+\Delta_n)+(1-\Delta_p)^{-1/3}(1-\Delta_n)\big] \\ & + \frac{\xi}{16}\frac{10}{9}[t_1+t_2] \\ & \times (1-\beta)^{5/3}(1+\beta)\big[(1+\Delta_p)^{-1/3}(1-\Delta_n)+(1-\Delta_p)^{-1/3}(1+\Delta_n)\big] \\ & - \frac{2\rho}{16}\Big[t_0(1-x_0)+\frac{1}{6}t_3(1-x_3)\rho^\gamma\Big](1-\beta)^2\Bigg\};\end{aligned} \tag{A.50}$$

$$\begin{aligned}\frac{1}{\chi_{np}} = \frac{1}{\chi_{pn}} = \frac{\rho}{\mu_n\rho_n\mu_p\rho_p}\Bigg\{ & \frac{\xi}{16}\frac{5}{3}[t_1x_1+t_2x_2] \\ & \times \Big[(1+\beta)^{5/3}(1-\beta)\big\{(1+\Delta_n)^{2/3}+(1-\Delta_n)^{2/3}\big\} \\ & + (1-\beta)^{5/3}(1+\beta)\big\{(1+\Delta_p)^{2/3}+(1-\Delta_p)^{2/3}\big\}\Big] \\ & + \frac{2\rho}{16}\Big[t_0x_0+\frac{1}{6}t_3x_3\rho^\gamma\Big](1-\beta^2)\Bigg\};\end{aligned} \tag{A.51}$$

# Bibliography


[1] S. Shapiro and S. Teukolsky, *Black Holes, White Dwarfs and Neutron Stars* (Wiley, New York, 1983).

[2] J. M. Lattimer and M. Prakash, Phys. Rep. **442**, 109 (2007).

[3] C. González-Boquera, M. Centelles, X. Viñas, and A. Rios, arXiv:1706.02736v1 [nucl-th].

[4] M. Baldo, *Nuclear Methods and the Nuclear Equation of State*, International Review of Nuclear Physics, Vol. 8 (World Scientific (Singapore), 1999).

[5] `http://nn-online.org`, a service created and maintained by the Theoretical High Energy Physics Group, Ranbout University Nijmegen, the Netherlands.

[6] H. Müther and A. Polls, Prog. Part. Nucl. Phys. **45**, 243 (2010).

[7] P. Ring and P. Schuck *The Nuclear Many-Body Problem* (Springer, New York, 1980).

[8] T. R. H. Skyrme, Nucl. Phys.**9**, 615 and 635 (1959).

[9] D. Vautherin and D. M. Brink, Phys. Rev. C **3**, 626 (1972).

[10] J. Dechargé and D. Gogny, Phys. Rev. C **21**, 1568 (1980).

[11] J. R. Stone and P.G. Reinhard, Prog. Part. Nucl. Phys. **58**, 587 (2007).

[12] P. G. Reinhard and H. Flocard, Nucl. Phys. A **584**, 467 (1995).

[13] J. Margueron, J. Navarro, and N. V. Giai, Phys. Rev. C **66**, 014303 (2002).

[14] J. R. Stone, J. C. Miller, R. Koncewicz, P. D. Stevenson, and M. R. Strayer, Phys. Rev. C **68**, 034324 (2003).

[15] E. Chabanat, P. Bonche, P. Hansel, J. Meyer, and R. Schaeffer, Nucl. Phys. A **627**, 710 (1997).

[16] E. Chabanat, P. Bonche, P. Hansel, J. Meyer, and R. Schaeffer, Nucl. Phys. A **635**, 231 (1998).

[17] R. B. Wiringa, V. Ficks, and A. Fabrocini, Phys. Rev. C **38**, 1010 (1988).

[18] R. Sellahewa and A. Rios, Phys. Rev. C **90**, 054327 (2014).

[19] J. P. Blaizot, J. F. Berger, J. Dechargé and M. Girod Nucl. Phys. A **591**, 435 (1995).

[20] F. Chappert, M. Girod, and S. Hilaire, Phys. Lett. B **668**, 420 (2008).

[21] S. Goriely, S. Hilaire, and M. Girod, and S. Péru, Phys. Rev. Lett. **102**, 242501 (2009).

[22] A. Rios, A. Polls, and I. Vidaña, Phys. Rev. C **71**, 055802 (2005).

[23] A. A. Isayev and J. Yang, Phys. Rev. C **69**, 025801 (2004).

[24] A. A. Isayev, Phys. Rev. C **74**, 057301 (2006).

[25] I. Vidaña, C. Providencia, A. Polls, and A. Rios, Phys. Rev. C **80**, 045806 (2009).

[26] X. Roca-Maza, M. Centelles, X. Viñas, and M. Warda, Phys. Rev. Lett. **106**, 252501 (2011).

[27] X. Viñas, M. Centelles, X. Roca-Maza, and M. Warda, Eur. Phys. J. A **50**, 27 (2014).

[28] M. Centelles, X. Roca-Maza, X. Viñas, and M. Warda, Phys. Rev. Lett. **102**, 122502 (2009).

[29] M. B. Tsang, *et. al.*, Phys. Rev. C **86**, 015803 (2012).

[30] D. López-Val, A. Rios, and A. Polls, I. Vidaña, Phys. Rev. C **74**, 068801 (2006).

[31] I. Vidaña and I. Bombaci, Phys. Rev. C **66**, 045801 (2002).

[32] N. K. Glendenning, *Compact stars: nuclear physics, particle physics, and general relativity*, 2nd ed., Astronomy and Astrophysics Library, Vol.242 (Springer (New York), 2000) pp. 313-332.

[33] F. Pacini, Nature (London) **216**, 567 (1967).

[34] T. Gold, Nature (London) **218**, 731 (1968).

[35] M. Prakash, I. Bombaci, Manju Prakash, P. J. Ellis, J. M. Lattimer, and R. Knorren, Phys. Rep. **280**, 1 (1997).

[36] J. Navarro, E. S. Hernández, and D. Vautherin, Phys. Rev. C **60**, 045801 (1999).

[37] I. Vidaña, A. Polls, and V. Durant, Phys. Rev. C **94**, 054006 (2016).

[38] A. Polls, V. Durant, and I, Vidaña, Acta Physica Polonica B Proceedings Supplement No1 Vol. 10 (2017).

[39] S. Fantoni, A. Sarsa, and K. E. Schmidt, Phys. Rev. Lett. **87**, 181101 (2001).

[40] I. Vidaña, A. Polls, and A. Ramos, Phys. Rev. C **65**, 035804 (2002).

[41] J. M. Pearson and G. Saunier, Phys. Rev. Lett. **24**, 325 (1970).

[42] S. Fantoni, A. Sarsa, and K. E. Schmidt, Phys. Rev. Lett. **87**, 181101 (2001).

[43] I. Bombaci, A. Polls, A. Ramos, A. Rios, and I. Vidaña, Phys. Lett. B **632**, 638 (2006).

[44] F. Sammarruca and P. G. Krastev, Phys. Rev. C **75**, 034315 (2007).

[45] F. Sammarruca, Phys. Rev. C **83**, 064304 (2011).

[46] B. Behera, X. Viñas, T. R. Routray, and M. Centelles, J. Phys. G: Nucl. Part. Phys. **42**, 045103 (2015).

[47] A. Vidaurre, J. Navarro, and J. Bernabeu, Astron. Astrophys. **135**, 361 (1984).

[48] N. Chamel and S. Goriely, Phys. Rev. C **82**, 045804 (2010).